

1 **Recent seismic activity at Cephalonia island (Greece): A**
2 **study through candidate electromagnetic precursors in**
3 **terms of nonlinear dynamics.**

4
5 **S. M. Potirakis**¹, **Y. Contoyiannis**², **N. S. Melis**³, **J. Kopanas**⁴,
6 **G. Antonopoulos**⁴, **G. Balasis**⁵, **C. Kontoes**⁵, **C. Nomicos**⁶, **K. Eftaxias**²

7
8 [1] {Department of Electronics Engineering, Piraeus University of Applied Sciences (TEI of
9 Piraeus), 250 Thivon and P. Ralli, Aigalao, Athens, GR-12244, Greece, spoti@teipir.gr }.

10 [2] {Department of Physics, Section of Solid State Physics, University of Athens,
11 Panepistimiopolis, GR-15784, Zografos, Athens, Greece,(Y. C: yconto@yahoo.gr ; K. E.:
12 ceftax@phys.uoa.gr)}

13 [3] {Institute of Geodynamics, National Observatory of Athens, Lofos Nimfon, Thissio,
14 Athens, GR-11810, Greece, nmelis@noa.gr}

15 [4] {Department of Environmental Technologists, Technological Education Institute (TEI) of
16 the Ionian islands, Zakynthos, GR-29100, Greece, (J. K.: jkopan@otenet.gr ; G. A.:
17 sv8rx@teiion.gr)}

18 [5] {Institute for Astronomy, Astrophysics, Space Applications and Remote Sensing, National
19 Observatory of Athens, Metaxa and Vasileos Pavlou, Penteli, Athens, GR-15236, Greece, (G.
20 B.:gbalasis@noa.gr ; C. K.: kontoes@noa.gr)}

21 [6] {Department of Electronics Engineering, Technological Education Institute (TEI) of
22 Athens, Ag. Spyridonos, Aigaleo, Athens, GR-12210, Greece, cnomicos@teiath.gr}

23

24 Correspondence to: G. Balasis (gbalasis@noa.gr)

25

1 **Abstract**

2 The preparation process of two recent earthquakes (EQs) occurred in Cephalonia (Kefalonia)
3 island, Greece, [(38.22° N, 20.53° E), 26 January 2014, $M_w=6.0$, depth = 21 km], and
4 [(38.25° N, 20.39° E), 3 February 2014, $M_w=5.9$, depth = 10 km], respectively, is studied in
5 terms of the critical dynamics revealed in observables of the involved non-linear processes.
6 Specifically, we show, by means of the method of critical fluctuations (MCF), that signatures
7 of critical, as well as tricritical, dynamics were embedded in the fracture-induced
8 electromagnetic emissions (EME) recorded by two stations in locations near the epicenters of
9 these two EQs. It is worth noting that both, the MHz EME recorded by the telemetric stations
10 on the island of Cephalonia and the neighboring island of Zante (Zakynthos), reached
11 simultaneously critical condition a few days before the occurrence of each earthquake. The
12 critical characteristics embedded in the EME signals were further verified using the natural
13 time (NT) method. Moreover, we show, in terms of the NT method, that the foreshock
14 seismic activity also presented critical characteristics before each one of these events.
15 Importantly, the revealed critical process seems to be focused on the area corresponding to the
16 west Cephalonia zone, following the seismotectonic and hazard zoning of the Ionian Islands
17 area near Cephalonia.

18

19 **Keywords:** Fracture-induced electromagnetic emissions; Earthquake dynamics; Criticality -
20 Tricriticality; Method of Critical Fluctuations; Natural Time Analysis; Seismotectonic Zone
21 Partitioning.

22

23 **1. Introduction**

24 The possible connection of the electromagnetic (EM) activity that is observed prior to
25 significant earthquakes (EQs) with the corresponding EQ preparation processes, often referred
26 to as seismo-electromagnetics, has been intensively investigated during the last years. Several
27 possible EQ precursors have been suggested in the literature (Uyeda et al., 2009a; Cicerone et
28 al., 2009; Hayakawa, 2013a, 2013b; Varotsos 2005; Varotsos et al., 2011b). The possible
29 relation of the field observed fracture-induced electromagnetic emissions (EME) in the
30 frequency bands of MHz and kHz, associated with shallow EQs with magnitude 6 or larger

1 that occurred in land or near coast, has been examined in a series of publications in order to
2 contribute to a better understanding of the underlying processes (e.g., [Eftaxias et al., 2001,](#)
3 [2004, 2008, 2013;](#) [Kapiris et al., 2004;](#) [Karamanos et al., 2006;](#) [Papadimitriou et al., 2008;](#)
4 [Contoyiannis et al., 2005, 2013, 2015;](#) [Eftaxias and Potirakis, 2013;](#) [Potirakis et al., 2011,](#)
5 [2012a, 2012b, 2012c, 2013, 2015;](#) [Minadakis et al., 2012a, 2012b](#)), while a four-stage model
6 for the preparation of an EQ by means of its observable EM activity has been recently put
7 forward ([Eftaxias and Potirakis, 2013, and references therein;](#) [Contoyiannis et al., 2015, and](#)
8 [references therein](#)). In summary, the proposed four stages of the last part of EQ preparation
9 process and the associated, appropriately identified, EM observables, specifically EM time
10 series excerpts for which specific features have been identified using appropriate time series
11 analysis methods, appear in the following order ([Donner et al., 2015, and references therein](#)):
12 1st stage: valid MHz anomaly; 2nd stage: kHz anomaly exhibiting tri-critical characteristics;
13 3rd stage: strong avalanche-like kHz anomaly; 4th stage: electromagnetic quiescence. It is
14 noted that, according to the aforementioned four-stage model, the pre-EQ MHz EME is
15 considered to be emitted during the fracture of the part of the Earth's crust that is
16 characterized by high heterogeneity. During this phase the fracture is non-directional and
17 spans over a large area that surrounds the family of large high-strength entities distributed
18 along the fault sustaining the system. Note that for an EQ of magnitude ~ 6 the corresponding
19 fracture process extends to a radius of ~ 120 km ([Bowman et al., 1998](#)).

20 Two strong shallow EQs occurred recently in western Greece (see Fig. 1). On 26 January
21 2014 (13:55:43 UT) an $M_w = 6.0$ EQ, hereafter also referred to as "EQ1", occurred on the
22 island of Cephalonia (Kefalonia), with epicenter at (38.22° N, 20.53° E) and depth of ~ 16 km.
23 The second significant EQ, $M_w = 5.9$, hereafter also referred to as "EQ2", occurred on the
24 same island on 3 February 2014 (03:08:45 UT), with epicenter at (38.25° N, 20.40° E) and
25 depth of ~ 11 km. Various studies of the two earthquakes have already been published
26 indicating their seismotectonic importance ([Karastathis et al., 2014;](#) [Valkaniotis et al., 2014;](#)
27 [Papadopoulos et al., 2014;](#) [Ganas et al., 2015;](#) [Sakkas and Lagios, 2015;](#) [Merryman Boncori et](#)
28 [al., 2015](#)) as they were located on two different active faults that belong to the same seismic
29 source zone.

30 Two pairs of MHz EM signals were recorded, with a sampling rate of 1 sample/s, prior to
31 each one of the above mentioned significant shallow EQs; one pair of simultaneous signals

1 was recorded by two different stations prior to each one of them. On 24 January 2014, two
2 days before the $M_w = 6.0$ Cephalonia EQ (EQ1), two telemetric stations of our EM signal
3 monitoring network (see Fig. 1), the station of Cephalonia, located on the same island (38.18°
4 N, 20.59° E), and the station of Zante (Zakynthos), located on a neighboring island belonging
5 to the same (Ionian) island complex (37.77° N, 20.74° E), simultaneously recorded the first
6 pair of aforementioned signals. The same picture was repeated for the second significant
7 Cephalonia EQ, $M_w = 5.9$ (EQ2). Specifically, both the Cephalonia and the Zante stations
8 simultaneously recorded the second pair of aforementioned signals on 28 January 2014, six
9 days prior to the specific EQ. Note that it has been repeatedly made clear that all the pre-EQ
10 EME signals, which have been observed by our monitoring network, have been recorded only
11 prior to strong shallow EQs, that have taken place on land (or near the coast-line); this fact, in
12 combination to the recently proposed fractal geo-antenna model (Eftaxias et al., 2004;
13 Eftaxias and Potirakis, 2013), explains why they succeed to be transmitted on air. This model
14 gives a good reason for the increased possibility of detection of such EM radiation, since a
15 fractal geo-antenna emits significantly increased power, compared to the power that would be
16 radiated by the same source, if a dipole antenna model was considered. It should also be noted
17 that, none of the recordings of the other monitoring stations of our network (except from the
18 ones of Cephalonia and Zante) presented critical characteristics before these two specific EQs.

19

20

<Figure 1 should be placed around here>

21

22 The analysis of the specific EM time series, using the method of critical fluctuations (MCF)
23 (Contoyiannis and Diakonos, 2000; Contoyiannis et al., 2002, 2013), revealed critical
24 features, implying that the possibly related underlying geophysical process was at critical
25 state before the occurrence of each one of the EQs of interest. The critical characteristics
26 embedded in the specific time series were further verified by means of the natural time (NT)
27 method (Varotsos et al., 2011a, 2011b, Potirakis et al., 2013, 2015). The presence of the
28 “critical point” during which any two active parts of the system are highly correlated,
29 theoretically even at arbitrarily long distances, in other words when “everything depends on
30 everything else”, is consistent with the view that the EQ preparation process during the period

1 that the MHz EME are emitted is a spatially extensive process. Note that this process
2 corresponds to the first stage of the aforementioned four-stage model.

3 Moreover, we analyzed the foreshock seismic activity using the NT method; the obtained
4 results indicate that seismicity also presented critical characteristics before each one of the
5 two important events. This result implies that the observed EM anomaly and the associated
6 foreshock seismic activity might be considered as “two sides of the same coin”. Last but not
7 least, one day before the occurrence of EQ2, and five days after the corresponding critical
8 EME signal, tricritical characteristics were revealed in the EME recorded by the Cephalonia
9 station.

10 The remainder of this manuscript is organized as follows: A brief introduction to the MCF
11 and the NT analysis methods is provided in Section 2. The analysis of the EME recordings
12 according to these two methods is presented in Section 3. Section 4 presents the results
13 obtained by the analysis of the foreshock seismic activity using the NT method, while Section
14 5 concludes the manuscript by summarizing and discussing the findings.

15

16 **2. Critical Dynamics Analysis Methods**

17 Criticality has early been suggested as an EQ precursory sign ([Chelidze, 1982](#); [Chelidze and](#)
18 [Kolesnikov, 1982](#); [Chelidze et al., 2006](#); [Rundle et al., 2012](#); [Wanliss et al., 2015](#)). Critical
19 phenomena have been proposed as the likely framework to study the origins of EQ related
20 EM fluctuations, suggesting that the theory of phase transitions and critical phenomena may
21 be useful in gaining insight to the mechanism of their complex dynamics ([Bowman et al.,](#)
22 [1998](#); [Contoyiannis et al., 2004a, 2005, 2015](#); [Varotsos et al., 2011a, 2011b](#)). One possible
23 reason for the appropriateness of this model may be the way in which correlations spread
24 through a disordered medium/ system comprised of subunits. From a qualitative / intuitive
25 perspective, according to the specific approach, initially single isolated activated parts emerge
26 in the system which, then, progressively grow and proliferate, leading to cooperative effects.
27 Local interactions evolve to long-range correlations, eventually extending along the entire
28 system. A key point in the study of dynamical systems that develop critical phenomena is the
29 identification of the “critical epoch” during which the “short-range” correlations evolve into
30 “long-range” ones. Therefore, the theory of phase transitions and critical phenomena seem to
31 be appropriate for the study of dynamical complex systems in which local interactions evolve

1 to long-range correlations, such as the disordered Earth's crust during the preparation of an
 2 EQ. Note that for an EQ of magnitude ~ 6 the corresponding fracture process extends to a
 3 radius of ~ 120 km (Bowman et al., 1998).

4 It is worth noting that key characteristics of a critical point in a phase transition of the second
 5 order are the existence of highly correlated fluctuations and scale invariance in the statistical
 6 properties. By means of experiments on systems presenting this kind of criticality as well as
 7 by appropriately designed numerical experiments, it has been confirmed that right at the
 8 "critical point" the subunits are highly correlated even at arbitrarily large "distance". At the
 9 critical state self-similar structures appear both in time and space. This fact is quantitatively
 10 manifested by power law expressions describing the distributions of spatial or temporal
 11 quantities associated with the aforementioned self-similar structures (Stanley, 1987, 1999).

12 The time series analysis methods employed in this paper for the evaluation of the MHz EME
 13 recordings and the seismicity around the Cephalonia island in terms of critical dynamics are
 14 briefly presented in the following. Specifically, the method of critical fluctuations (MCF) is
 15 described in Sub-Section 2.1, while the natural time (NT) method is described in Sub-Section
 16 2.2.

17

18 **2.1 Method of critical fluctuations (MCF)**

19 In the direction of comprehending the dynamics of a system undergoing a continuous phase
 20 transition at critical state, the method of critical fluctuations (MCF) has been proposed for the
 21 analysis of critical fluctuations in the systems' observables (Contoyiannis and Diakonou,
 22 2000; Contoyiannis et al., 2002). The dynamics of various dynamical systems have been
 23 successfully analyzed by MCF; these include thermal (e.g., 3D Ising) (Contoyiannis et al.,
 24 2002), geophysical (Contoyiannis and Eftaxias 2008; Contoyiannis et al., 2004a, 2010, 2015),
 25 biological (electro-cardiac signals) (Contoyiannis et al., 2004b; Contoyiannis et al., 2013) and
 26 economic systems (Ozun et al., 2014).

27 It has been shown (Contoyiannis and Diakonou, 2000) that the dynamics of the order
 28 parameter fluctuations ϕ at the critical state for a second-order phase transition can be
 29 theoretically formulated by the non-linear intermittent map:

$$30 \quad \phi_{n+1} = \phi_n + u\phi_n^z, \quad (1)$$

1 where ϕ_n is the scaled order parameter value at the time interval n ; u denotes an effective
 2 positive coupling parameter describing the non-linear self-interaction of the order parameter;
 3 z stands for a characteristic exponent associated with the isothermal exponent δ for critical
 4 systems at thermal equilibrium ($z = \delta + 1$). The marginal fixed-point of the above map is the
 5 zero point, as expected from critical phenomena theory.

6 However, it has been shown that in order to quantitatively study a real (or numerical)
 7 dynamical system one has to add an unavoidable “noise” term, ε_n , to Eq. (1), which is
 8 produced by all stochastic processes (Contoyiannis and Diakonou, 2007). Note that, from the
 9 intermittency mathematical framework point of view, the “noise” term denotes ergodicity in
 10 the available phase space. In this respect, the map of Eq. (1), for positive values of the order
 11 parameter, becomes:

$$12 \quad \phi_{n+1} = \left| \phi_n + u\phi_n^z + \varepsilon_n \right|. \quad (2)$$

13 Based on the map of Eq. (2), MCF has been introduced as a method capable of identifying
 14 whether a system is in critical state of intermittent type by analyzing time-series
 15 corresponding to an observable of the specific system. In a few words, MCF is based on the
 16 property of maps of intermittent-type, like the ones of Eqs. (1) and (2), that the distribution of
 17 properly defined laminar lengths (waiting times) l follow a power-law $P(l) \sim l^{-p_l}$ (Schuster,
 18 1998), where the exponent p_l is $p_l = 1 + \frac{1}{\delta}$ (Contoyiannis et al., 2002). However, the
 19 distribution of waiting times for a real data time series which is not characterized by critical
 20 dynamics follows an exponential decay, rather than a power-law one (Contoyiannis et al.,
 21 2004a), due to stochastic noise and finite size effects. Therefore, the dynamics of a real time
 22 series can be estimated by fitting the distribution of waiting times (laminar lengths) to a
 23 function $\rho(l)$ combining both power-law and exponential decay (Contoyiannis and Diakonou,
 24 2007):

$$25 \quad \rho(l) \sim l^{-p_2} e^{-lp_3}. \quad (3)$$

26 The values of the two exponents p_2 and p_3 , which result after fitting laminar lengths
 27 distribution in a log-log scale diagram, reveal the underlying dynamics. Exact critical state
 28 calls for $p_3 = 0$; in such a case it is $p_2 = p_l > 1$. As a result, in order for a real system to be

1 considered to be at critical state, *both criticality conditions* $p_2 > 1$ *and* $p_3 \approx 0$ *have to be*
 2 *satisfied.*

3 Note that the choice of the function $\rho(l)$ of Eq. (3), which combines both power-law and
 4 exponential decay, to model the distribution of waiting times was deliberately made in order
 5 to include both these fundamentally different behaviors, i.e., the critical dynamics
 6 (Contoyiannis et al., 2002) and the complete absence of specific dynamics (stochastic
 7 processes) (Contoyiannis et al., 2004b), respectively. Of course, the specific function also
 8 models intermediate behaviors (Contoyiannis and Diakonou, 2007).

9 In applying the MCF the corresponding factors of $\rho(l)$ appear to be competitive: any increase
 10 of the p_2 exponent value corresponds to a p_3 exponent value reduction and vice versa.
 11 However, this is expected because, for example, any increase of the value of p_3 exponent
 12 signifies the departure from critical dynamics and thus the reduction of p_2 exponent value.
 13 What is interesting to us is to apply MCF analysis to observe this competition in the case of
 14 pre-earthquake EME time-series and see whether the obtained exponent values are consistent
 15 with those of MCF analyzes performed on other time-series with large statistics which are
 16 considered as references for the application of our method. This competition can be observed
 17 even within the critical windows as shown in Figs. 2d and 3d.

18 Moreover, a special dynamics case is the one known as “tricritical crossover dynamics”. In
 19 statistical physics, a tricritical point is a point in the phase diagram of a system at which the
 20 two basic kinds of phase transition, that is the first order transition and the second order
 21 transition, meet (Huang, 1987). A characteristic property of the area around this point is the
 22 co-existence of three phases, specifically, the high symmetry phase, the low symmetry phase,
 23 and an intermediate “mixing state”. A passage through this area, around the tricritical point,
 24 from the second order phase transition to the first order phase transition through the
 25 intermediate mixing state constitutes a tricritical crossover (Huang, 1987).

26 The specific dynamics is proved to be expressed by the map (Contoyiannis et al., 2015):

$$27 \quad m_{n+1} = \left| m_n - u m_n^{-z} + \varepsilon_n \right|, \quad (4)$$

28 where m stands for the order parameter. This map differs from the critical map of Eq. (2) in
 29 the sign of the parameter u and exponent z . Note that for reasons of unified formulation we

1 use for these parameters the same notation as in the critical map of Eq. (2). At the level of
 2 MCF analysis this dynamics is expressed by the estimated values for the two characteristic
 3 exponents p_2, p_3 values, that satisfy *the tricriticality condition* $p_2 < 1, p_3 \approx 0$. These values
 4 have been characterized in (Contoyiannis and Diakonou, 2007) as a signature of tricritical
 5 behavior.

6 Note that in order for a time-series to be possible to be analyzed by the MCF, it should at least
 7 present cumulative stationarity. Therefore, a cumulative stationarity test is always performed
 8 before applying the MCF method; examples can be found in already published articles (e.g.,
 9 Contoyiannis et al., 2004a, 2005, 2010; Contoyiannis and Eftaxias, 2008; Potirakis et al.,
 10 2015). More details on the application of MCF can be found in several published articles
 11 (e.g., Contoyiannis et al. 2002, 2013, 2015), as well as in Section 3 where its application on
 12 the MHz EM variations is presented.

13

14 **2.2 Natural time method (NT)**

15 The natural time method was originally proposed for the analysis for a point process like DC
 16 or ultra-low frequency (≤ 1 Hz) SES (Varotsos et al., 2002; Varotsos, 2005), and has been
 17 shown to be optimal for enhancing the signals in the time-frequency space (Abe et al., 2005).
 18 The transformation of a time-series of “events” from the conventional time domain to natural
 19 time domain is performed by ignoring the time-stamp of each event and retaining only their
 20 normalized order (index) of occurrence. Explicitly, in a time series of N successive events,
 21 the natural time, χ_k , of the k^{th} event is the index of occurrence of this event normalized, by
 22 dividing by the total number of the considered events, $\chi_k = k/N$. On the other hand, the
 23 “energy”, Q_k , of each, k^{th} , event is preserved. We note that the quantity Q_k represents
 24 different physical quantities for various time series: for EQ time series it has been assigned to
 25 a seismic energy released (e.g., seismic moment) (Varotsos et al., 2005; Uyeda et al., 2009b),
 26 and for SES signals that are of dichotomous nature it corresponds to SES pulse duration
 27 (Varotsos, 2005), while for MHz electromagnetic emission signals that are of non-
 28 dichotomous nature, it has been attributed to the energy of fracto-electromagnetic emission
 29 events as defined in Potirakis et al. (2013). The transformed time series (χ_k, Q_k) is then

1 studied through the normalized power spectrum $\Pi(\varpi) = \left| \sum_{k=1}^N p_k \exp(j\varpi\chi_k) \right|^2$, where ϖ is
 2 the natural angular frequency, $\varpi = 2\pi\varphi$, with φ standing for the frequency in natural time,
 3 termed “natural frequency”, and $p_k = Q_k / \sum_{n=1}^N Q_n$ corresponds to the k^{th} event’s normalized
 4 energy. Note that, the term “natural frequency” should not be confused with the rate at which
 5 a system oscillates when it is not driven by an external force; it defines an analysis domain
 6 dual to the natural time domain, in the framework of Fourier–Stieltjes transform (Varotsos et
 7 al., 2011b).

8 The study of $\Pi(\varpi)$ at ϖ close to zero reveals the dynamic evolution of the time series under
 9 analysis. This is because all the moments of the distribution of p_k can be estimated from
 10 $\Pi(\varpi)$ at $\varpi \rightarrow 0$ (Varotsos et al., 2011a). Aiming to that, by the Taylor expansion
 11 $\Pi(\varpi) = 1 - \kappa_1 \varpi^2 + \kappa_2 \varpi^4 + \dots$, the quantity κ_1 is defined, where
 12 $\kappa_1 = \sum_{k=1}^N p_k \chi_k^2 - \left(\sum_{k=1}^N p_k \chi_k \right)^2$, i.e., the variance of χ_k weighted for p_k characterizing the
 13 dispersion of the most significant events within the “rescaled” interval $(0,1]$. Moreover, the
 14 entropy in natural time, S_{nt} , is defined (Varotsos et al., 2006) as
 15 $S_{nt} = \sum_{k=1}^N p_k \chi_k \ln \chi_k - \left(\sum_{k=1}^N p_k \chi_k \right) \ln \left(\sum_{k=1}^N p_k \chi_k \right)$ and corresponds (Varotsos et al., 2006,
 16 2011b) to the value at $q=1$ of the derivative of the fluctuation function $F(q) = \langle \chi^q \rangle - \langle \chi \rangle^q$
 17 with respect to q (while κ_1 corresponds to $F(q)$ for $q=2$). It is a dynamic entropy
 18 depending on the sequential order of events (Varotsos et al., 2006). The entropy, S_{nt-} ,
 19 obtained upon considering (Varotsos et al., 2006) the time reversal T , i.e., $Tp_m = p_{N-m+1}$, is
 20 also considered.

21 A system is considered to approach criticality when the parameter κ_1 converges to the value
 22 $\kappa_1 = 0.070$ and at the same time both the entropy in natural time and the entropy under time
 23 reversal satisfy the condition $S_{nt}, S_{nt-} < S_u = (\ln 2/2) - 1/4$ (Sarlis et al., 2011), where S_u
 24 stands for the entropy of a “uniform” distribution in natural time (Varotsos et al., 2006).

1 In the special case of natural time analysis of foreshock seismicity (Varotsos et al., 2001,
2 2005,2006; Sarlis et al., 2008), the seismicity is considered to be in a true critical state, a “true
3 coincidence” is achieved, when three additional conditions are satisfied: (i) The “average”
4 distance $\langle D \rangle$ between the curves of normalized power spectra $\Pi(\varpi)$ of the evolving
5 seismicity and the theoretical estimation of $\Pi(\varpi)$,

$$6 \quad \Pi_{critical}(\varpi) = (18/5\varpi^2) - (6\cos\varpi/5\varpi^2) - (12\sin\varpi/5\varpi^3), \quad \Pi_{critical}(\varpi) \approx 1 - \kappa_1\varpi^2, \text{ for}$$

7 $\kappa_1 = 0.070$ should be smaller than 10^{-2} , i.e., $\langle D \rangle = \langle |\Pi(\varpi) - \Pi_{critical}(\varpi)| \rangle < 10^{-2}$; (ii) the
8 parameter κ_1 should approach the value $\kappa_1 = 0.070$ “by descending from above” (Varotsos et
9 al., 2001); (iii) Since the underlying process is expected to be self-similar, the time of the true
10 coincidence should not vary upon changing (within reasonable limits) either the magnitude
11 threshold, M_{thres} , or the area, used in the calculation.

12 It should be finally clarified that in the case of seismicity analysis, the temporal evolution of
13 the parameters κ_1 , S_{nt} , S_{nt-} , and $\langle D \rangle$ is studied as new events that exceed the magnitude
14 threshold M_{thres} are progressively included in the analysis. Specifically, as soon as one more
15 event is included, first the time series (χ_k, Q_k) is rescaled in the natural time domain, since
16 each time the k^{th} event corresponds to a natural time $\chi_k = k/N$, where N is the
17 progressively increasing (by each new event inclusion) total number of the considered
18 successive events; then all the parameters involved in the natural time analysis are calculated
19 for this new time series; this process continues until the time of occurrence of the main event.

20 More details on the application of NT on MHz EME as well as on foreshock seismicity can be
21 found in already published articles (Potirakis et al. 2013, 2015), as well as in Sections 3 and 4,
22 where its application on the MHz EM variations and foreshock seismicity is presented,
23 respectively.

24 Note that in the case of NT analysis of foreshock seismicity, the introduction of magnitude
25 threshold, M_{thres} , excludes some of the weaker EQ events (with magnitude below this
26 threshold) from the NT analysis. On one hand, this is necessary in order to exclude events for
27 which the recorded magnitude is not considered reliable; depending on the installed
28 seismographic network characteristics, a specific magnitude threshold is usually defined to

1 assure data completeness. On the other hand, the use of various magnitude thresholds, M_{thres} ,
 2 offers a means of more accurate determination of the time when criticality is reached. In some
 3 cases, it happens that more than one time-points may satisfy the rest of NT critical state
 4 conditions, however the time of the true coincidence is finally selected by the last condition
 5 that “true coincidence should not vary upon changing (within reasonable limits) either the
 6 magnitude threshold, M_{thres} , or the area, used in the calculation.”

7 **3. Electromagnetic Emissions Analysis Results**

8 Part of the MHz recordings of the Cephalonia station associated with the $M_w = 6.0$ EQ (EQ1)
 9 is shown in Fig. 2a. This was recorded in day of year 24, that is ~2 days before the occurrence
 10 of EQ1. This stationary time series excerpt, having a total length of 2.8 h (10,000 samples)
 11 starting at 24 Jan. 2014 (12:46:40 UT), was analyzed by the MCF method and was identified
 12 to be a “critical window” (CW). CWs are time intervals of the MHz EME signals presenting
 13 features analogous to the critical point of a second order phase transition (Contoyiannis et al.,
 14 2005).

15 The main steps of the MCF analysis (e.g., Contoyiannis et al., 2013, 2015) on the specific
 16 time series are shown in Fig. 2b- Fig. 2d. First, a distribution of the amplitude values of the
 17 analyzed signal was obtained from which, using the method of turning points (Pingel et al.,
 18 1999), a fixed-point, that is the start of laminar regions, ϕ_o of about 700 mV was determined.
 19 Fig. 2c portrays the obtained distribution of laminar lengths for the end point $\phi_l = 655mV$,
 20 that is the distribution of waiting times, referred to as laminar lengths l , between the fixed-
 21 point ϕ_o and the end point ϕ_l , as well as the fitted function $f(l) \propto l^{-p_2} e^{-p_3 l}$ with the
 22 corresponding exponents $p_2 = 1.35$, $p_3 = 0.000$ with $R^2 = 0.999$. Note that the distribution
 23 of laminar lengths is directly fitted to the specific model using the Levenberg-Marquardt
 24 algorithm, while the fitting criterion is the chi-square minimization. The fitting is not done in
 25 log-log space; the axes of Fig. 2c are logarithmic for the easier depiction of the distribution of
 26 laminar lengths. Finally, Fig. 2d shows the obtained plot of the p_2, p_3 exponents vs. ϕ_l . From
 27 Fig. 2d it is apparent that the criticality conditions, $p_2 > 1$ and $p_3 \approx 0$, are satisfied for a wide
 28 range of end points ϕ_l , revealing the power-law decay feature of the time series that proves

1 that the system is characterized by intermittent dynamics; in other words, the MHz time series
2 excerpt of Fig. 2a is indeed a CW.

3

4 <Figure 2 should be placed around here>

5

6 Part of the MHz recordings of the Zante station associated with EQ1 is shown in Fig. 3a. This
7 was also recorded in day of year 24, that is ~2 days before the occurrence of Cephalonia EQ1.
8 This stationary time series excerpt, having a total length of 2.8 h (10,000 samples) starting at
9 24 Jan. 2014 (12:46:40 UT), was also analyzed by the MCF method and was identified to be a
10 “critical window” (CW).

11 The application of the MCF analysis on the specific time series (cf. Fig. 3), revealed that the
12 criticality conditions, $p_2 > 1$ and $p_3 \approx 0$, are satisfied for a wide range of end points ϕ_l , for
13 this signal too. In other words, this signal has also embedded the power-law decay feature that
14 indicates intermittent dynamics, rendering it a CW..

15 <Figure 3 should be placed around here>

16

17 After the $M_w = 6.0$ (EQ1), ~ a week later, the second, $M_w = 5.9$ (EQ2), occurred on the
18 same island with a focal area a few km further than the first one. Six days earlier, both the
19 Cephalonia and Zante stations simultaneously recorded MHz EME. Specifically, a stationary
20 time series excerpt, having a total length of 3.3 h (12,000 samples) starting at 28 Jan. 2014
21 (05:33:20 UT), from Caphalonia station and a stationary time series excerpt, having a total
22 length of 5 h (18,000 samples) starting at 28 Jan. 2014 (03:53:20 UT), from Zante station
23 were analyzed by the MCF method and both of them were identified to be CWs. Note that the
24 Cephalonia CW was emitted within the time frame in which the Zante CW was emitted. Figs
25 4 & 5 show the results of the corresponding analyses.

26

27 <Figure 4 should be placed around here>

28

1 <Figure 5 should be placed around here>

2

3 In summary, we conclude that, according to the MCF analysis method, both stations recorded
4 MHz signals that simultaneously presented critical state features two days before the first
5 main event and six days before the second main event. In order to verify this finding, we
6 proceeded to the analysis of all the corresponding MHz signals by means of the NT analysis
7 method, according to the way of application proposed in Potirakis et al. (2013). According to
8 the specific procedure for the application of the NT method on the MHz signals, we
9 performed an exhaustive search seeking for at least one amplitude threshold value (applied
10 over the total length of the analyzed signal), for which the corresponding fracto-EME events
11 satisfy the natural time method criticality conditions. The idea is that if the MCF gives valid
12 information, and as a consequence the analyzed time series excerpt is indeed in critical
13 condition, then there should be at least one threshold value for which the NT criticality
14 conditions (cf. Sec. 2.2) are satisfied. Indeed, as apparent from Fig. 6, all four signals satisfy
15 the criticality conditions according to the NT method for at least one of the considered
16 threshold values, therefore the results obtained by the MCF method are successfully verified.

17

18 <Figure 6 should be placed around here>

19

20 On 2 February 2014, i.e., one day before the occurrence of EQ2, MHz EME presenting
21 tricritical characteristics was recorded by the Cephalonia station. This signal emerged five
22 days after the CWs that were identified in the simultaneously recorded, by the Cephalonia and
23 Zante stations, MHz EME. The specific MHz time series excerpt from Cephalonia station,
24 having a total length of 7.5 h (27,000 samples) starting at 2 Feb. 2014 (07:46:40 UT), was
25 analyzed by means of the MCF method yielding the results shown in Fig. 7. As apparent from
26 the results, this signal satisfies the tricriticality conditions $p_2 < 1, p_3 \approx 0$ (cf. Sec. 2.1) for a
27 wide range of end points ϕ , revealing the intermediate “mixing state” between the second
28 order phase transition to the first order phase transition. Unfortunately, during the time that
29 the Cephalonia station recorded tricritical MHz signal, the Zante station was out of order;
30 actually, it was out of order for several hours during the specific day.

1
2
3
4
5
6
7
8
9
10
11
12
13
14
15
16
17
18
19
20
21
22
23
24
25
26
27
28

<Figure 7 should be placed around here>

It has been recently found (Contoyiannis et al., 2015) that such a behavior is identified in the kHz EME which usually emerge near the end of the MHz EME when the environment in which the EQ preparation process evolves changes from heterogeneous to less heterogeneous, and before the emergence of the strong avalanche-like kHz EME which have been attributed to the fracture of the asperities sustaining the fault. Actually, this has been proposed as the second stage of the four-stage model for the preparation of an EQ by means of its observable EM activity (Eftaxias and Potirakis, 2013, and references therein; Contoyiannis et al., 2015, and references therein; Donner et al., 2015). The identification of tricritical behavior in MHz EME is a quite important finding, indicating that the tricritical behavior, attributed to the second stage of the aforementioned four-stage model, can be identified either in kHz or in MHz EME, leading thus to a revision the specific four-stage model in order to include this case too.

As a conclusion, after the first stage of the EQ preparation process where MHz EME with critical features are emitted, a second stage follows where MHz or kHz or both MHz and kHz EME with tricritical features are emitted. As already mentioned (cf. Sec. 2.1), in terms of statistical physics the tricritical behavior is an intermediate dynamical state which is developed in region of the phase diagram of a system around the tricritical point, which can be approached either from the edge of the first order phase transition (characterizing the strong avalanche-like kHz EME attributed to the third stage of the four-stage model) or from the edge of the second order phase transition (characterizing the critical MHz EME attributed to the first stage of the four-stage model). Therefore, although it is expected that the tricritical behavior will be rarely observed, as it has already been discussed in (Contoyiannis et al., 2015), it can be found either in MHz time series, following the emission of a critical MHz EME, or in kHz time series preceding the emission of avalanche-like kHz EME.

4. Foreshock Seismic Activity Analysis Results

1 **4. Foreshock Seismic Activity Analysis Results**
2 As already mentioned in Potirakis et al. (2013, 2015): “seismicity and pre-fracture EMEs
3 should be two sides of the same coin concerning the EQ generation process. If the MHz
4 EMEs and the corresponding foreshock seismic sequence are observable manifestations of the
5 same complex system at critical state, both should be possible to be described as a critical
6 phenomenon by means of the natural time method.” Therefore, we also proceeded to the
7 examination of the corresponding foreshock seismic activity around Cephalonia before each
8 one of the significant EQs of interest in order to verify this suggestion. However, we did not
9 apply the NT method on concentric circles around the epicenter of each EQ, as in Potirakis et
10 al. (2013, 2015), but instead we decided to study seismicity within areas determined
11 according to seismotectonic and earthquake hazard criteria.

12 Following the detailed study presented in Vamvakaris et al. (2016), we incorporated the
13 seismic zones proposed there for our area of study. Thus, as it is presented in Fig. 8, we
14 defined five separate seismic zones, based on the criteria explored in Vamvakaris et al. (2016)
15 and the seismic zonation proposed by them. Since the study area, comprises the most
16 seismically active zone in Greece, assigned also the highest value on the Earthquake Building
17 Code for the country, a large number of source, stress and strain studies have been used in
18 their study to establish such definition of zoning. Hence, it was found well justified to follow
19 their zone definition. In Fig. 8, from east to west and north to south, one can identify the
20 zones of Akarnania (area no. 1), Lefkada island (area no. 2), east Cephalonia island (area no.
21 3), west Cephalonia island (area no. 4), and Zante island (area no. 5), respectively, covering
22 the area of the Ionian Sea near Cephalonia island.

23

24 <Figure 8 should be placed around here>

25

26 Before we proceed to the NT analysis of seismicity, the seismic activity prior to EQ1, as well
27 as between EQ1 and EQ2 is briefly discussed in relation to the above mentioned seismic
28 zones. Earthquake parametric data have been retrieved from the National Observatory of
29 Athens on-line catalogue (<http://www.gein.noa.gr/en/seismicity/earthquake-catalogs>), while
30 for all the presented maps and calculations the local magnitude (M_L), as provided by the

1 specific earthquake catalog, is used. The foreshock seismic activity before EQ1 for the whole
 2 investigated area of the Ionian Sea region from 13 December 2013 up to the time of
 3 occurrence of the main event is shown in the map of Fig. 9a. As it can be easily observed
 4 from this map, there was a high seismic activity mainly focused on two specific zones: west
 5 Cephalonia and Zante. Notably, an EQ of $M_L = 4.7$ occurred in Zante on 11/01/2014
 6 04:12:58, indicated by the black arrow in Fig. 9a. No EQs were recorded in Akarnania, while
 7 very few events were recorded in Lefkada and east Cephalonia. The events which occurred in
 8 west Cephalonia are also shown in a separate map in Fig. 9b for later reference.

9

10 <Figure 9 should be placed around here>

11

12 Applying the natural time analysis on seismic data (cf. Sec. 2.2), the evolution of the time
 13 series (χ_k, Q_k) was studied for the foreshock seismicity prior to EQ1, where Q_k is in this
 14 case the seismic energy released during the k^{th} event. The seismic moment, M_0 , as
 15 proportional to the seismic energy, is usually considered (Varotsos et al., 2005; Uyeda et al.,
 16 2009b; Potirakis et al., 2013,2015). Our calculations were based on the seismic moment M_0
 17 (in dyn.cm) resulting from the corresponding M_L as (Varotsos et al., 2005; Potirakis et al.,
 18 2013, 2015), $M_0 = 10^{0.99M_L + 11.8}$. First, we performed an NT analysis on the seismicity activity
 19 of the whole investigated Ionian Sea region during the period from 13/12/2013 00:00:00 to
 20 26/01/2014 13:55:44 UT, i.e., just after the occurrence of EQ1, for different magnitude
 21 thresholds, M_{thres} , for which all earthquakes having $M_L > M_{thres}$ were included in the analysis.
 22 Note that, only $M_{thres} \geq 2$ was considered in order to assure data completeness (Chouliaras et
 23 al., 2013a, 2013b).

24 For all the considered threshold values, the result was the same: no indication of criticality
 25 was identified (see for example Fig. 10a). Since, as we have already mentioned, the whole
 26 investigated area was mainly dominated by the seismic activity in west Cephalonia and the
 27 seismic activity in Zante, while an EQ of $M_L = 4.7$ occurred in Zante, we decided to start the
 28 NT analysis after the occurrence of the specific Zante EQ, in order to exclude from our
 29 analysis possible foreshock activity related to the specific event. As a result, we performed

1 NT analysis for the time period 11/01/2014 04:13:00 (just after the $M_L = 4.7$ Zante EQ) to
2 26/01/2014 13:55:44 UT, for different magnitude thresholds in three successively enclosed
3 areas: namely, the whole investigated area of Ionian Islands region, both Cephalonia (east and
4 west) zones combined, and the zone of west Cephalonia. Representative examples of these
5 analyses are depicted in Fig. 10b – Fig. 10d. The analysis over the whole investigated area of
6 the Ionian Islands region indicates that seismicity reaches criticality on 19 and 20 of January,
7 while the two other progressively narrower areas indicate that the criticality conditions
8 according to NT method are satisfied on 19 and 22 of January. These results imply that
9 seismicity was also in critical condition a few days prior to the occurrence of the first studied
10 significant Cephalonia EQ (EQ1). Actually, in the specific case, the critical condition of
11 seismicity was reached before, but quite close, to the emission of the corresponding MHz
12 signals for which critical behavior was identified (cf. Sec. 3). Note that a very recent analysis
13 on the foreshock seismic activity before EQ1, in terms of a combination of multiresolution
14 wavelets and NT analysis, which was performed on concentric areas of 50 km and 30 km
15 radii around the epicenter of EQ1, also found that NT analysis criticality requirements are met
16 a few days before EQ1 (at approximately 20 January) (Vallianatos et al., 2015).

17

18 <Figure 10 should be placed around here>

19

20 Before the application of the NT method to the seismic activity prior to EQ2, one should first
21 study the time evolution of the activity between the two significant events of interest, in order
22 to minimize if possible the influence of the first EQ aftershock sequence on the NT analysis.
23 Our first observation about the EQs which occurred during the specific time period was that,
24 all but one had epicenters in west Cephalonia. Only one $M_L = 2.3$ EQ occurred in Zante, at
25 (37.79° N, 21.00° E) on 28 January 2014 02:08:27 UT.

26 Fig. 11a shows all the events that were recorded in the whole investigated area of the Ionian
27 Islands region vs. time from just after EQ1 ($M_w = 6.0$) up to the time of EQ2 ($M_w = 5.9$),
28 including EQ2. As it can be seen, if one considers that both significant EQs of interest were
29 main events, it is quite difficult to separate the seismic activity of the specific time period into
30 aftershocks of the first EQ and foreshocks of the second one. However, we observe that up to

1 a specific time point, there is a rapid decrease of the running mean magnitude of the recorded
2 EQs, while after that the long range (75 events) running mean value seems to be almost
3 constant over time with the short range (25 events) one varying around it. We arbitrarily set
4 the 29 January 00:00:00 UT as the time point after which the recorded seismicity is no longer
5 dominated by the aftershocks of EQ1; this by no means implies that the aftershock sequence
6 of the EQ1 stops after that date. It should also be underlined that changing this, arbitrarily
7 selected, date within reasonable limits, does not significantly changes the results of our
8 corresponding NT analysis which are presented next. On the other hand, a significant shift of
9 this limit towards EQ1, i.e., to earlier dates, results to severe changes indicating the
10 domination of the recorded seismicity by the aftershock sequence of EQ1. Accordingly, the
11 considered as foreshock seismic activity before EQ2, i.e., from 29/01/2014 00:00 UT up to
12 the time of occurrence of EQ2, is presented in the map of Fig. 11b for west Cephalonia and
13 analyzed in the following.

14

15 <Figure 11 should be placed around here>

16

17 Next, we applied the NT method on the seismicity of west Cephalonia for the time period
18 from 29/01/2014 00:00:00 to 03/02/2014 03:08:47 UT. Note that we also applied the NT
19 method on the whole investigated area of the Ionian Islands region, obtaining practically the
20 same results. As we have already mentioned, only one $M_L = 2.3$ EQ occurred outside the
21 west Cephalonia zone, so, on the one hand for magnitude threshold values $M_{thres} \geq 2.3$ this
22 event was excluded, while, on the other hand, even for lower threshold values
23 ($2 \leq M_{thres} < 2.3$) its inclusion does not change the results significantly. Fig. 12 shows the NT
24 analysis results for some threshold values proving that seismicity reaches criticality on 1 or 2
25 February 2014, that is one or two days before the occurrence of the second significant EQ of
26 interest ($M_w = 5.9$). Actually, in the specific case, the critical condition of seismicity was
27 reached after, but quite close, to the emission of the corresponding MHz signals for which
28 critical behavior was identified (cf. Sec. 3).

29

1 <Figure 12 should be placed around here>

2

3

5. Discussion - Conclusions

4

Based on the methods of critical fluctuations and natural time, we have shown that the fracture-induced MHz EME recorded by two stations in our network prior to two recent significant EQs occurred in Cephalonia present criticality characteristics, implying that they emerge from a system in critical state.

8

There are two key points that render these observations unique in the up to now research on the pre-EQ EME:

9

10 (i) The Cephalonia station is known for being insensitive to EQ preparation processes
11 happening outside of the wider area of Cephalonia island, as well as to EQ preparation
12 processes leading to low magnitude EQs within the area of Cephalonia island. Note that the
13 only signal that has been previously recorded refers to the M=6 EQ that occurred on the
14 specific island in 2007 ([Contoyiannis et al., 2010](#)).

15 (ii) Prior to each one of the studied significant EQs, two MHz EME time series presenting
16 critical characteristics were recorded simultaneously in two different stations very close to the
17 focal areas, while no other station of our network (cf. Fig. 1) recorded such signals prior to the
18 specific EQs. This indicates that the revealed criticality was not associated with a global
19 phenomenon, such as critical variations in the Ionosphere, but was rather local to the area of
20 the Ionian Islands region, enhancing the hypothesis that these EME were associated with the
21 EQ preparation process taking place prior to the two significant EQs. This feature, combined
22 with the above mentioned sensitivity of the Cephalonia station only to significant EQs
23 occurring on the specific island, could have been considered as an indication of the location of
24 the impending EQs.

25 EME, as a phenomenon rooted in the damage process, should be an indicator of memory
26 effects. Laboratory studies verify that: during cyclic loading, the level of EME increases
27 significantly when the stress exceeds the maximum previously reached stress level (Kaizer
28 effect). The existence of Kaizer effect predicts the EM silence during the aftershock period
29 ([Eftaxias et al., 2013](#); [Eftaxias and Potirakis, 2013](#), and references therein). Thus, the

1 appearance of the second EM anomaly may reveal that the corresponding preparation of
2 fracture process has been organized in a new barrier.

3 We note that, according to the view that seismicity and pre-EQ EM emissions should be “two
4 sides of the same coin” concerning the earthquake generation process, the corresponding
5 foreshock seismic activity, as another manifestation of the same complex system, should be at
6 critical state as well, before the occurrence of a main event. We have shown that this really
7 happens for both significant EQs we studied. Importantly, the revealed critical process seems
8 to be focused on an area corresponding to the west Cephalonia zone, one of the parts
9 according to the seismotectonic and hazard zone partitioning of the wider area of the Ionian
10 Islands.

11 To be more detailed, the foreshock seismicity associated with the first ($M_w = 6.0$) EQ
12 reached critical condition a few days before the occurrence of the main event. Specifically, it
13 came to critical condition before, but quite close, to the emission of the corresponding MHz
14 signals for which critical behavior was identified. The seismicity that was considered as
15 foreshock of the second ($M_w = 5.9$) EQ also reached criticality few days before the
16 occurrence of the main event. In contrary to the first EQ case, it came to criticality after, but
17 quite close, to the emission of the corresponding MHz signals for which critical behavior was
18 identified.

19 One more outcome of our study was the identification of tricritical crossover dynamics in the
20 MHz emissions recorded just before the occurrence of the second significant EQ of interest
21 ($M_w = 5.9$) at the Cephalonia station. Note that, unfortunately, the Zante station was out of
22 order for several hours during the specific day, including the time window during which the
23 tricritical features were identified in the Cephalonia recordings. As a result, we could not
24 cross check whether tricritical signals simultaneously also reached Zante. This is considered a
25 quite important finding, since it verifies a theoretically expected situation, namely the
26 approach of the intermediate dynamical state of tricritical crossover, either from the first or
27 from the second order phase transition state. In terms of pre-EQ EME, this leads to a revision
28 of the four-stage model for the preparation of an EQ by means of its observable EM activity.
29 Namely, after the first stage of the EQ preparation process where MHz EME with critical
30 features are emitted, a second stage follows where MHz or kHz or both MHz and kHz EME
31 with tricritical features are emitted. Specifically, the tricritical crossover dynamics can be

1 identified either in MHz time series, following the emission of a critical MHz EME, or in kHz
2 time series preceding the emission of avalanche-like kHz EME. In summary, the proposed
3 four stages of the last part of EQ preparation process and the associated, appropriately
4 identified, EM observables appear in the following order: 1st stage: valid MHz anomaly; 2nd
5 stage: MHz or kHz or MHz and kHz anomaly exhibiting tri-critical characteristics; 3rd stage:
6 strong avalanche-like kHz anomaly; 4th stage: electromagnetic quiescence. Note that the
7 specific four-stage model is a suggestion that seems to be verified by the up to now available
8 MHz-kHz observation data and corresponding time-series analyzes, while a rebuttal has not
9 yet appeared in the literature. However, the understanding of the physical processes involved
10 in the preparation of an EQ and their relation to various available observables is an open
11 scientific issue. Much effort still remains to be paid before one can claim clear understanding
12 of EQ preparation processes and associated possible precursors.

13 As it has been repeatedly pointed out in previous works (e.g., [Eftaxias et al., 2013](#); [Eftaxias](#)
14 [and Potirakis, 2013](#), and references therein), our view is that such observations and the
15 associated analyses offer valuable information for the comprehension of the Earth system
16 processes that take place prior to the occurrence of a significant EQ. As it is known, a large
17 number of other precursory phenomena are also observed, both by ground and satellite
18 stations, prior to significant EQs. Only a combined evaluation of our observations with other
19 well documented precursory phenomena could possibly render our observations useful for a
20 reliable short-term forecast solution. Unfortunately, in the cases of the Cephalonia EQs under
21 study this requirement was not fulfilled. To the best of our knowledge, only one paper
22 reporting the emergence of VLF seismic-ionospheric disturbances four days before the first
23 Cephalonia EQ ([Skeberis et al., 2015](#)) has been published up to now. It is very important that
24 the specific disturbances, which also correspond to a spatially extensive process as happens
25 with the MHz EME, were recorded during the same time window with the here presented
26 MHz critical signals. However, more precursory phenomena could have been investigated if
27 appropriate observation data were available. For example, if ground-based magnetic
28 observatories in the area of Greece had available magnetometer data for the time period of
29 interest, EQ-related ULF magnetic field variations, either of lithospheric or ionospheric
30 origin, which are also a result of spatially extensive processes and in other cases have been
31 shown to present critical characteristics prior to EQ occurrence ([Hayakawa et al., 2015](#)), could
32 also be investigated.

1

2 **Acknowledgements**

3 The authors S. M. P., Y. C., N. S. M., J. K., G. A., C. N. and K. E. would like to acknowledge
4 that this research was co-funded by the EU (European Social Fund) and national funds, action
5 “Archimedes III—Funding of research groups in T.E.I.”, under the Operational Programme
6 “Education and Lifelong Learning 2007-2013”. The authors G. B. and C. K. would like to
7 acknowledge support from the European Union Seventh Framework Programme (FP7-
8 REGPOT-2012-2013-1) under grant agreement no. 316210 (BEYOND – Building Capacity
9 for a Centre of Excellence for EO-based monitoring of Natural Disasters).

10

11 **REFERENCES**

- 12 Abe, S., Sarlis, N. V., Skordas, E. S., Tanaka, H. K., Varotsos, P. A.: Origin of the usefulness
13 of the natural-time representation of complex time series, *Phys. Rev. Lett.*, 94, doi:
14 10.1103/PhysRevLett.94.170601, 2005.
- 15 Bowman, D., Ouillon, G., Sammis, C., Sornette, A., Sornette, D.: An observational test of the
16 critical earthquake concept, *J. Geophys. Res.*, 103, 24359-24372, doi:
17 10.1029/98JB00792, 1998.
- 18 Chelidze, T.: Percolation and fracture, *Phys. Earth Planet. In.*, 28, 93-101, 1982.
- 19 Chelidze, T., Kolesnikov, Yu. M.: Percolation modell des bruchprozesses, *Gerlands Beitr.*
20 *Geophysik. Leipzig*, 91, 35-44, 1982.
- 21 Chelidze, T., Kolesnikov, Yu., Matcharashvili, T.: Seismological criticality concept and
22 percolation model of fracture, *Geophys. J. Int.*, 164, 125-136, 2006.
- 23 Chouliaras, G., Melis, N. S., Drakatos, G., Makropoulos, K.: Operational network
24 improvements and increased reporting in the NOA (Greece) seismicity catalog,
25 *Geophysical Research Abstracts*, 15, EGU2013-12634-6., 2013a.
- 26 Chouliaras, G., Melis, N. S., Drakatos, G., Makropoulos, K.: Operational network
27 improvements and increased reporting in the NOA (Greece) seismicity catalog, *Adv.*
28 *Geosci.*, 36, 7-9, doi: 10.5194/adgeo-36-7-2013, 2013b.
- 29 Cicerone, R. D., Ebel, J. E., Britton, J.: A systematic compilation of earthquake precursors,
30 *Tectonophysics*, 476, 371-396, doi: 10.1016/j.tecto.2009.06.008, 2009.
- 31 Contoyiannis, Y., Diakonou, F.: Criticality and intermittency in the order parameter space,
32 *Phys. Lett. A*, 268, 286 -292, doi: 10.1016/S0375-9601(00)00180-8, 2000.
- 33 Contoyiannis, Y., Diakonou, F., Malakis, A.: Intermittent dynamics of critical fluctuations,
34 *Phys. Rev. Lett.*, 89, 035701, doi: 10.1103/PhysRevLett.89.035701, 2002.

- 1 Contoyiannis, Y. F., Diakonos, F. K., Kapiris, P. G., Peratzakis, A. S., Eftaxias, K. A.:
2 Intermittent dynamics of critical pre-seismic electromagnetic fluctuations, *Phys.*
3 *Chem. Earth*, 29, 397-408, doi: 10.1016/j.pce.2003.11.012, 2004a.
- 4 Contoyiannis, Y. F., Diakonos, F. K., Papaefthimiou, C., Theophilidis, G.: Criticality in the
5 relaxation phase of a spontaneously contracting atria isolated from a Frog's Heart,
6 *Phys. Rev. Lett.*, 93, 098101, doi: 10.1103/PhysRevLett.93.098101, 2004b.
- 7 Contoyiannis, Y. F., Kapiris, P. G., Eftaxias, K. A.: A Monitoring of a pre-seismic phase from
8 its electromagnetic precursors, *Phys. Rev. E*, 71, 066123, 066123/1-14, doi:
9 10.1103/PhysRevE.71.066123, 2005.
- 10 Contoyiannis, Y. F., Diakonos, F. K.: Unimodal maps and order parameter fluctuations in the
11 critical region, *Phys. Rev. E*, 76, 031138, 2007.
- 12 Contoyiannis, Y. F., Eftaxias, K.: Tsallis and Levy statistics in the preparation of an
13 earthquake, *Nonlin. Processes Geophys.*, 15, 379-388, doi:10.5194/npg-15-379-
14 2008, 2008.
- 15 Contoyiannis, Y. F., Nomicos, C., Kopanas, J., Antonopoulos, G., Contoyianni, L., Eftaxias,
16 K.: Critical features in electromagnetic anomalies detected prior to the L'Aquila
17 earthquake, *Physica A*, 389, 499-508, doi: 10.1016/j.physa.2009.09.046, 2010.
- 18 Contoyiannis, Y. F., Potirakis, S. M., Eftaxias, K.: The Earth as a living planet: human-type
19 diseases in the earthquake preparation process, *Nat. Hazards Earth Syst. Sci.*, 13,
20 125-139, doi: 10.5194/nhess-13-125-2013, 2013.
- 21 Contoyiannis, Y., Potirakis, S. M., Eftaxias, K., Contoyianni, L.: Tricritical crossover in
22 earthquake preparation by analyzing preseismic electromagnetic emissions, *J.*
23 *Geodynamics*, 84, 40-54, doi: 10.1016/j.jog.2014.09.015, 2015.
- 24 Donner, R. V., Potirakis, S. M., Balasis, G., Eftaxias, K., Kurths, J.: Temporal correlation
25 patterns in pre-seismic electromagnetic emissions reveal distinct complexity profiles
26 prior to major earthquakes, *Phys. Chem. Earth*, In Press (on-line available), doi:
27 10.1016/j.pce.2015.03.008, 2015.
- 28 Eftaxias, K., Kapiris, P., Polygiannakis, J., Bogris, N., Kopanas, J., Antonopoulos, G.,
29 Peratzakis, A., Hadjicontis, V.: Signatures of pending earthquake from electromagnetic
30 anomalies, *Geophys. Res. Lett.*, 28, 3321-3324, doi: 10.1029/2001GL013124, 2001.
- 31 Eftaxias, K., Frangos, P., Kapiris, P., Polygiannakis, J., Kopanas, J., Peratzakis, A.,
32 Skountzos, P., Jaggard, D.: Review and a model of pre-seismic electromagnetic
33 emissions in terms of fractal electrodynamics, *Fractals*, 12, 243-273, doi:
34 10.1142/S0218348X04002501, 2004.
- 35 Eftaxias, K., Contoyiannis, Y., Balasis, G., Karamanos, K., Kopanas, J., Antonopoulos, G.,
36 Koulouras, G., Nomicos, C.: Evidence of fractional-Brownian-motion-type asperity
37 model for earthquake generation in candidate pre-seismic electromagnetic emissions,
38 *Nat. Hazards Earth Syst. Sci.*, 8, 657-669, doi:10.5194/nhess-8-657-2008, 2008.

- 1 Eftaxias, K., Potirakis, S. M., Chelidze, T.: On the puzzling feature of the silence of
2 precursory electromagnetic emissions, *Nat. Hazards Earth Syst. Sci.*, 13, 2381-2397,
3 doi: 10.5194/nhess-13-2381-2013, 2013.
- 4 Eftaxias, K., Potirakis, S. M.: Current challenges for pre-earthquake electromagnetic
5 emissions: shedding light from micro-scale plastic flow, granular packings, phase
6 transitions and self-affinity notion of fracture process, *Nonlin. Processes Geophys.*, 20,
7 771–792, doi:10.5194/npg-20-771-2013, 2013.
- 8 Ganas, A., Cannavo, F., Chousianitis, K., Kassaras, I., Drakatos, G.: Displacements recorded
9 on continuous GPS stations following the 2014 M6 Cephalonia (Greece) earthquakes:
10 Dynamic characteristics and kinematic implications, *Acta Geodyn. Geomater.*, 12(1), 5–
11 27, doi: 10.13168/AGG.2015.0005, 2015.
- 12 Hayakawa, M. (ed.): *The Frontier of Earthquake Prediction Studies*, Nihon-Senmontosho-
13 Shuppan, Tokyo, 2013a.
- 14 Hayakawa, M. (ed.): *Earthquake Prediction Studies: Seismo Electromagnetics*, Terrapub,
15 Tokyo, 2013b.
- 16 Hayakawa, M., Schekotov, A., Potirakis, S. and Eftaxias, K.: Criticality features in ULF
17 magnetic fields prior to the 2011 Tohoku earthquake, *Proc. Japan Acad., Ser. B*, 91,
18 25-30, doi: 10.2183/pjab.91.25, 2015.
- 19 Huang, K.: *Statistical Mechanics*, 2nd Ed. John Wiley and sons, New York, 1987.
- 20 Kapiris, P., Eftaxias, K., Chelidze, T.: Electromagnetic signature of prefracture criticality in
21 heterogeneous media, *Phys. Rev. Lett.*, 92(6), 065702/1-4, doi:
22 10.1103/PhysRevLett.92.065702, 2004.
- 23 Karamanos, K., Dakopoulos, D., Aloupis, K., Peratzakis, A., Athanasopoulou, L.,
24 Nikolopoulos, S., Kapiris, P., Eftaxias, K.: Study of pre-seismic electromagnetic signals
25 in terms of complexity, *Phys. Rev. E*, 74, 016104/1-21, doi:
26 10.1103/PhysRevE.74.016104, 2006.
- 27 Karastathis, V. K., Mouzakiotis, E., Ganas, A., Papadopoulos, G. A.: High-precision
28 relocation of seismic sequences above a dipping Moho: The case of the January-
29 February 2014 seismic sequence in Cephalonia Isl. (Greece), *Solid Earth Discuss.*, 6,
30 2699-2733, doi: 10.5194/sed-6-2699-2014, 2014.
- 31 Merryman Boncori, J. P., Papoutsis, I., Pezzo, G., Tolomei, C., Atzori, S., Ganas, A.,
32 Karastathis, V., Salvi, S., Kontoes, C., Antonioli, A.: The February 2014 Cephalonia
33 earthquake (Greece): 3D deformation field and source modeling from multiple SAR
34 techniques, *Seismol. Res. Lett.* 86(1), 1-14, doi: 10.1785/0220140126, 2015.
- 35 Minadakis, G., Potirakis, S. M., Nomicos, C., Eftaxias, K.: Linking electromagnetic
36 precursors with earthquake dynamics: an approach based on nonextensive fragment and
37 self-affine asperity models, *Physica A*, 391, 2232-2244, doi:
38 10.1016/j.physa.2011.11.049, 2012a.
- 39 Minadakis, G., Potirakis, S. M., Stonham, J., Nomicos, C., Eftaxias, K.: The role of
40 propagating stress waves in geophysical scale: Evidence in terms of nonextensivity,
41 *Physica A*, 391(22), 5648-5657, doi:10.1016/j.physa.2012.04.030, 2012b.
- 42 Ozun, A., Contoyiannis, Y. F., Diakonos, F. K., Haniyas, M., Magafas, L.: Intermittency in
43 stock market dynamic, *J. Trading* 9(3), 26-33, 2014.

- 1 Papadimitriou, K., Kalimeri, M., Eftaxias, K.: Nonextensivity and universality in the
2 earthquake preparation process, *Phys. Rev. E*, 77, 036101/1-14, doi:
3 10.1103/PhysRevE.77.036101, 2008.
- 4 Papadopoulos, G. A., Karastathis, V. K., Koukouvelas, I., Sachpazi, M., Baskoutas, I.,
5 Chouliaras, G., Agalos, A., Daskalaki, E., Minadakis, G., Moshou, A., Mouzakiotis, A.,
6 Orfanogiannaki, K., Papageorgiou, A., Spanos, D., Triantafyllou, I.: The Cephalonia,
7 Ionian Sea (Greece), sequence of strong earthquakes of January-February 2014: a first
8 report, *Res. Geoph.*, 4:5441, 19-30, doi:10.4081/rg.2014.5441, 2014.
- 9 Pingel, D., Schmelcher, P., Diakonou, F. K.: Theory and examples of the inverse Frobenius-
10 Perron problem for complete chaotic maps, *Chaos*, 9, 357-366, doi: 10.1063/1.166413,
11 1999.
- 12 Potirakis, S. M., Minadakis, G., Nomicos, C., Eftaxias, K.: A multidisciplinary analysis for
13 traces of the last state of earthquake generation in preseismic electromagnetic
14 emissions, *Nat. Hazards and Earth Syst. Sci.*, 11, 2859-2879, doi:10.5194/nhess-11-
15 2859-2011, 2011.
- 16 Potirakis, S. M., Minadakis, G., Eftaxias, K.: Analysis of electromagnetic pre-seismic
17 emissions using Fisher information and Tsallis entropy, *Physica A*, 391, 300-306,
18 doi:10.1016/j.physa.2011.08.003, 2012a.
- 19 Potirakis, S. M., Minadakis, G., Eftaxias, K.: Sudden drop of fractal dimension of
20 electromagnetic emissions recorded prior to significant earthquake, *Nat. Hazards*, 64,
21 641-650, doi:10.1007/s11069-012-0262-x, 2012b.
- 22 Potirakis, S. M., Minadakis, G., Eftaxias, K.: Relation between seismicity and pre-earthquake
23 electromagnetic emissions in terms of energy, information and entropy content, *Nat.*
24 *Hazards Earth Syst. Sci.*, 12, 1179-1183, doi:10.5194/nhess-12-1179-2012, 2012c.
- 25 Potirakis, S.M., Karadimitrakis, A. and Eftaxias, K.: Natural time analysis of critical
26 phenomena: the case of pre-fracture electromagnetic emissions, *Chaos*, 23, 2, 023117.
27 doi:10.1063/1.4807908, 2013.
- 28 Potirakis, S. M., Contoyiannis, Y., Eftaxias, K., Koulouras, G., and Nomicos, C.: Recent field
29 observations indicating an earth system in critical condition before the occurrence of a
30 significant earthquake, *IEEE Geosc. Remote Sens. Lett.*, 12(3), 631-635, doi:
31 10.1109/LGRS.2014.2354374, 2015.
- 32 Rundle, J. B., Holliday, J. R., Graves, W. R., Turcotte, D. L., Tiampo, K. F., Klein, W.:
33 Probabilities for large events in driven threshold systems, *Phys. Rev. E*, 86, 021106,
34 2012.
- 35 Sakkas, V., Lagios, E.: Fault modelling of the early-2014 ~ M6 Earthquakes in Cephalonia
36 Island (W. Greece) based on GPS measurements, *Tectonophysics*, 644-645, 184-196,
37 doi: 10.1016/j.tecto.2015.01.010, 2015.
- 38 Sarlis, N. V., Skordas, E. S., Varotsos, P. A.: Similarity of fluctuations in systems exhibiting
39 self-organized criticality, *Europhys. Lett.*, 96, 2, doi:10.1209/0295-5075/96/28006,
40 2011.
- 41 Sarlis, N. V., Skordas, E. S., Lazaridou, M. S., Varotsos, P. A.: Investigation of seismicity
42 after the initiation of a Seismic Electric Signal activity until the main shock, *Proc. Japan*
43 *Acad., Ser. B.*, 84, 331-343, 2008.

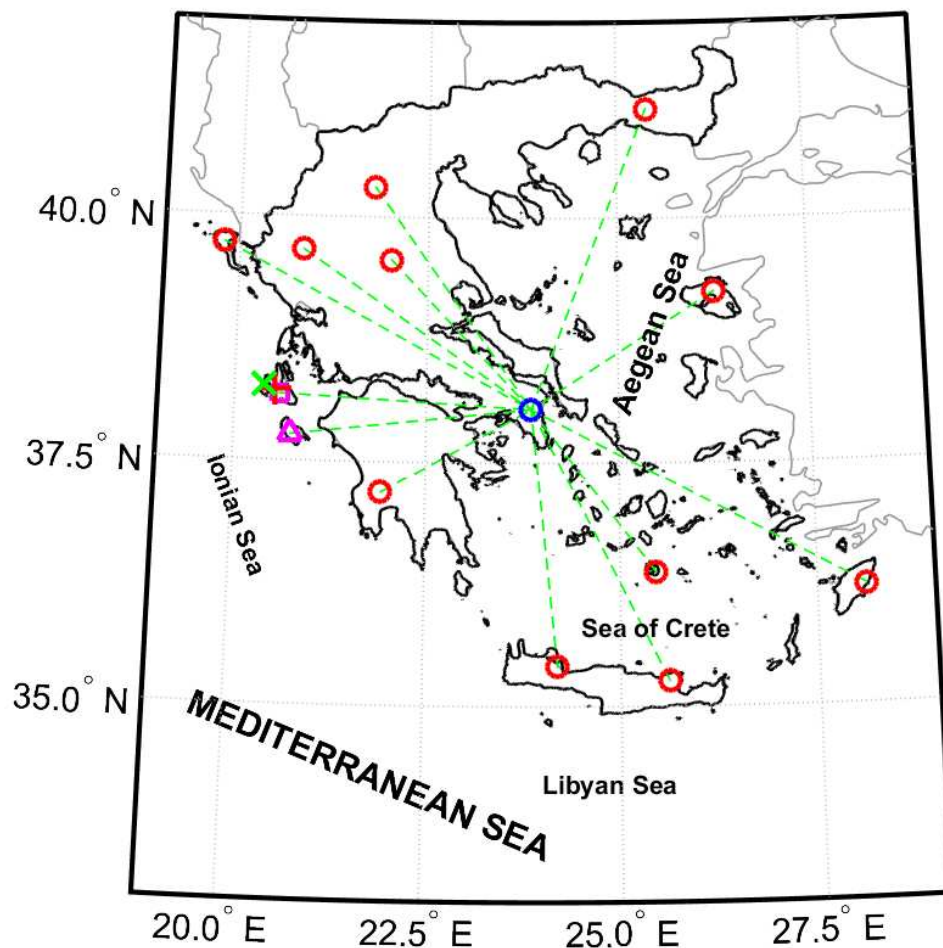
- 1 Schuster, H.: *Deterministic Chaos*, VCH, Weinheim, 1998.
- 2 Skeberis, C., Zaharis, Z.D., Xenos, T.D., Spatalas, S., Arabelos, D.N., Contadakis, M.E.:
3 Time–frequency analysis of VLF for seismic-ionospheric precursor detection:
4 Evaluation of Zhao-Atlas-Marks and Hilbert-Huang Transforms, *Phys. Chem. Earth*,
5 85-86, 174–184, doi:10.1016/j.pce.2015.02.006, 2015.
- 6 Stanley, H. E.: *Introduction to Phase Transitions and Critical Phenomena*, Oxford University
7 Press, New York, 1987.
- 8 Stanley, H. E.: Scaling, universality, and renormalization: Three pillars of modern critical
9 phenomena, *Rev. Modern Phys.*, 71, S358-S366, 1999.
- 10 Uyeda, S., Nagao, T., Kamogawa, M.: Short-term EQ prediction: Current status of seismo-
11 electromagnetics, *Tectonophysics*, 470, 205–213, 2009a.
- 12 Uyeda, S., Kamogawa, M., Tanaka, H.: Analysis of electrical activity and seismicity in the
13 natural time domain for the volcanic-seismic swarm activity in 2000 in the Izu Island
14 region, Japan, *J. Geophys Res.*, 114(B2), B02310, doi:10.1029/2007JB005332, 2009b.
- 15 Valkaniotis, S., Ganas, A., Papathanassiou, G., Papanikolaou, M.: Field observations of
16 geological effects triggered by the January-February 2014 Cephalonia (Ionian Sea,
17 Greece) earthquakes, *Tectonophysics*, 630, 150-157, doi: 10.1016/j.tecto.2014.05.012,
18 2014.
- 19 Vallianatos, F., Michas, G., Hloupis, G.: Multiresolution wavelets and natural time analysis
20 before the January-February 2014 Cephalonia (Mw6.1 & 6.0) sequence of strong
21 earthquake events, *Phys. Chem. Earth*, 85-86, 201–209, 2015.
- 22 Vamvakaris, D. A., Papazachos, C. B., Papaioannou, Ch. A., Scordilis, E. M., and Karakaisis,
23 G. F.: A detailed seismic zonation model for shallow earthquakes in the broader Aegean
24 area, *Nat. Hazards Earth Syst. Sci.*, 16, 55-84, doi:10.5194/nhess-16-55-2016, 2016.
- 25 Varotsos, P. A.: *The Physics of Seismic Electric Signals*, TERRAPUB, Tokyo, 2005.
- 26 Varotsos, P. A., Sarlis, N. V., Skordas, E. S.: Spatio-temporal complexity aspects on the
27 interrelation between seismic electric signals and seismicity., *Pract. Athens Acad.*, 76,
28 294-321, 2001.
- 29 Varotsos, P. A., Sarlis, N. V., Skordas, E. S.: Long-range correlations in the electric signals
30 that precede rupture, *Phys. Rev. E*, 66, 011902.doi:10.1103/ PhysRevE.66.011902,
31 2002.
- 32 Varotsos, P. A., Sarlis, N. V., Tanaka, H. K., Skordas, E. S.: Similarity of fluctuations in
33 correlated systems: The case of seismicity, *Phys. Rev. E*, 72, 041103. doi:
34 10.1103/PhysRevE.72.041103, 2005.
- 35 Varotsos, P. A., Sarlis, N. V., Skordas, E. S., Tanaka, H. K., Lazaridou, M. S.: Entropy of
36 seismic electric signals: Analysis in the natural time under time reversal, *Phys. Rev. E*,
37 73, 031114. doi:10.1103/PhysRevE.73.031114, 2006.
- 38 Varotsos, P., Sarlis, N., Skordas, E., Uyeda, S., Kamogawa, M.: Natural time analysis of
39 critical phenomena, *Proc. Natl. Acad. Sci. USA*, 108, 11361–11364, 2011a.
- 40 Varotsos, P., Sarlis, N., Skordas, E. S.: *Natural Time Analysis: The New View of Time*,
41 Springer, Berlin, 2011b.

- 1 Wanliss, J., Muñoz, V., Pastén, D., Toledo, B., Valdivia, J. A.: Critical behavior in earthquake
- 2 energy dissipation, *Nonlin. Processes Geophys. Discuss.*, 2, 619–645, 2015.

1

2 **Figures**

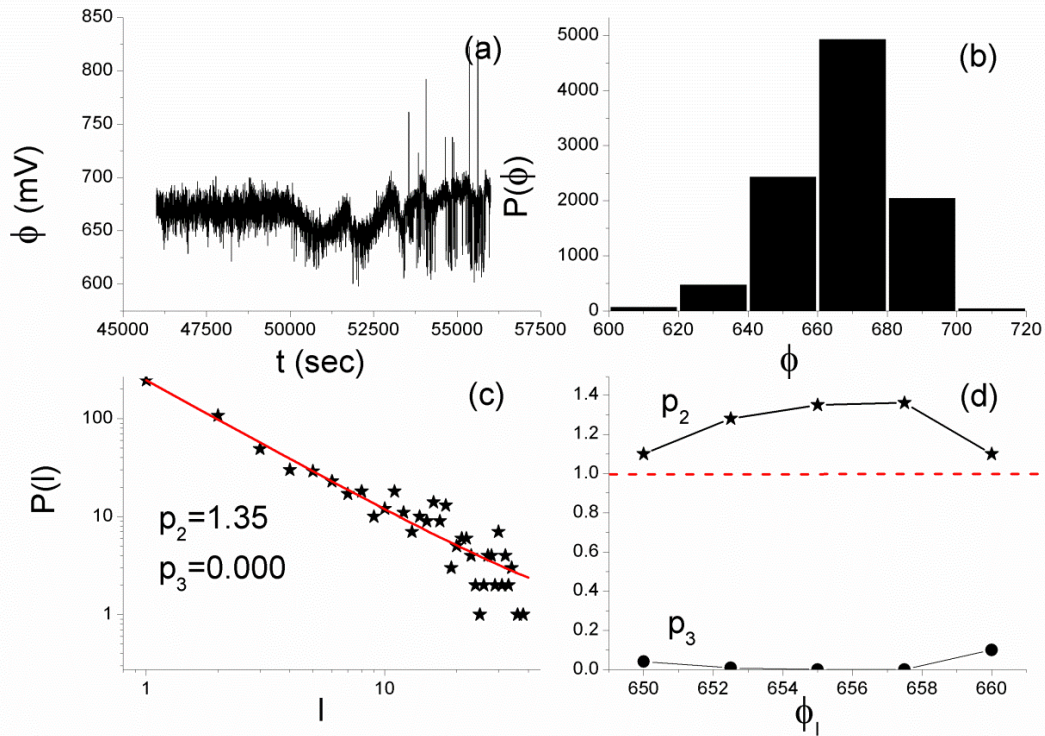
3



4

5 **Figure 1.** Map with distribution of stations of the telemetric network that monitors
6 electromagnetic variations in the MHz and kHz bands in Greece, which were operating during
7 the time period of interest. The locations of the Cephalonia and Zante stations are marked by
8 the magenta square and triangle, respectively, while the rest of the remote stations are denoted
9 by red circles and the central data recording server by a blue circle. The epicenters of the two
10 significant EQs of interest are also marked, the first (EQ1, $M_w = 6.0$) by a red cross and the
11 second (EQ2, $M_w = 5.9$) by a green X mark. (For interpretation of the references to colors,
12 the reader is referred to the online version of this paper.)

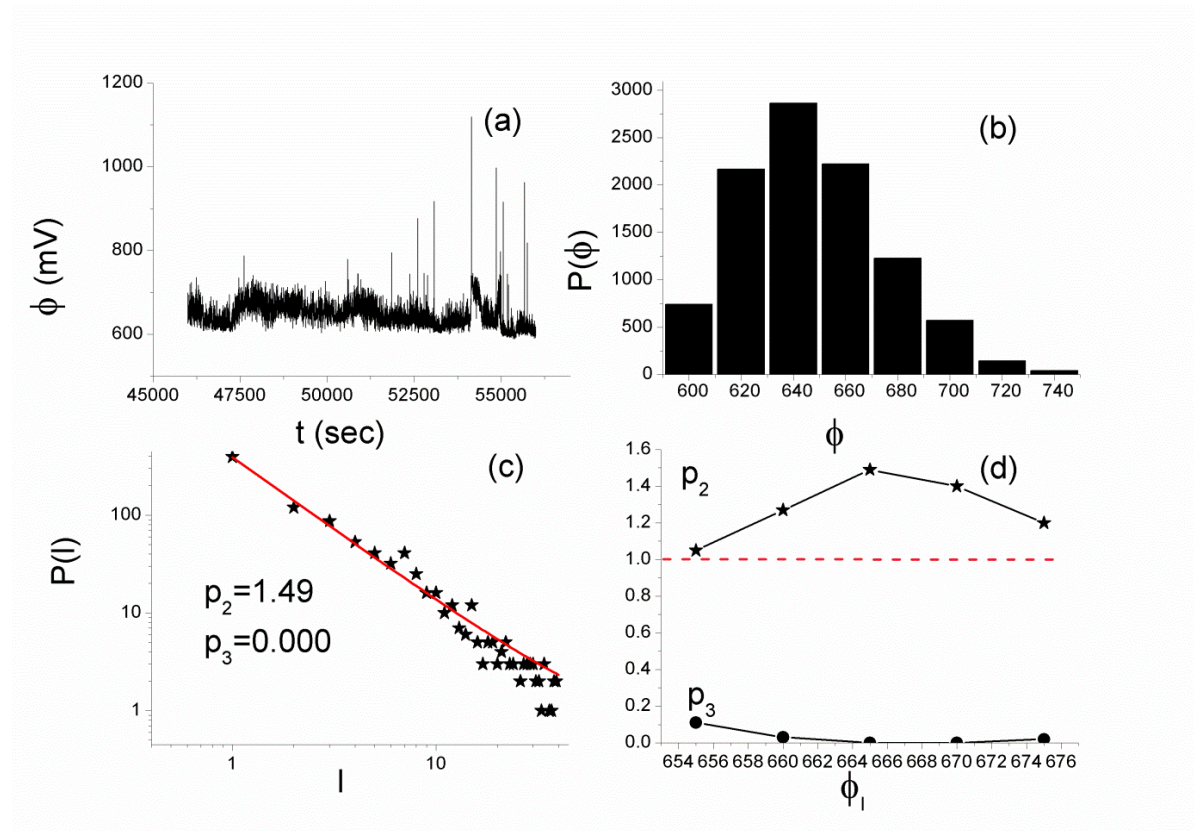
1



2

3 **Figure 2.** (a) The 10,000 samples long critical window of the MHz EME that was recorded
 4 before the Cephalonia $M_w = 6.0$ EQ at the Cephalonia station. (b) Amplitude distribution of
 5 the signal of Fig. 2a. (c) Distribution of laminar lengths for the end point $\phi_l = 655mV$, as a
 6 representative example of the involved fitting. The solid line corresponds to the fitted function
 7 (cf. to text in Sec. 2.1) with the values of the corresponding exponents p_2, p_3 also noted. (d)
 8 The obtained exponents p_2, p_3 vs. different values of the end of laminar region ϕ_l . The
 9 horizontal dashed line indicates the critical limit ($p_2 = 1$).

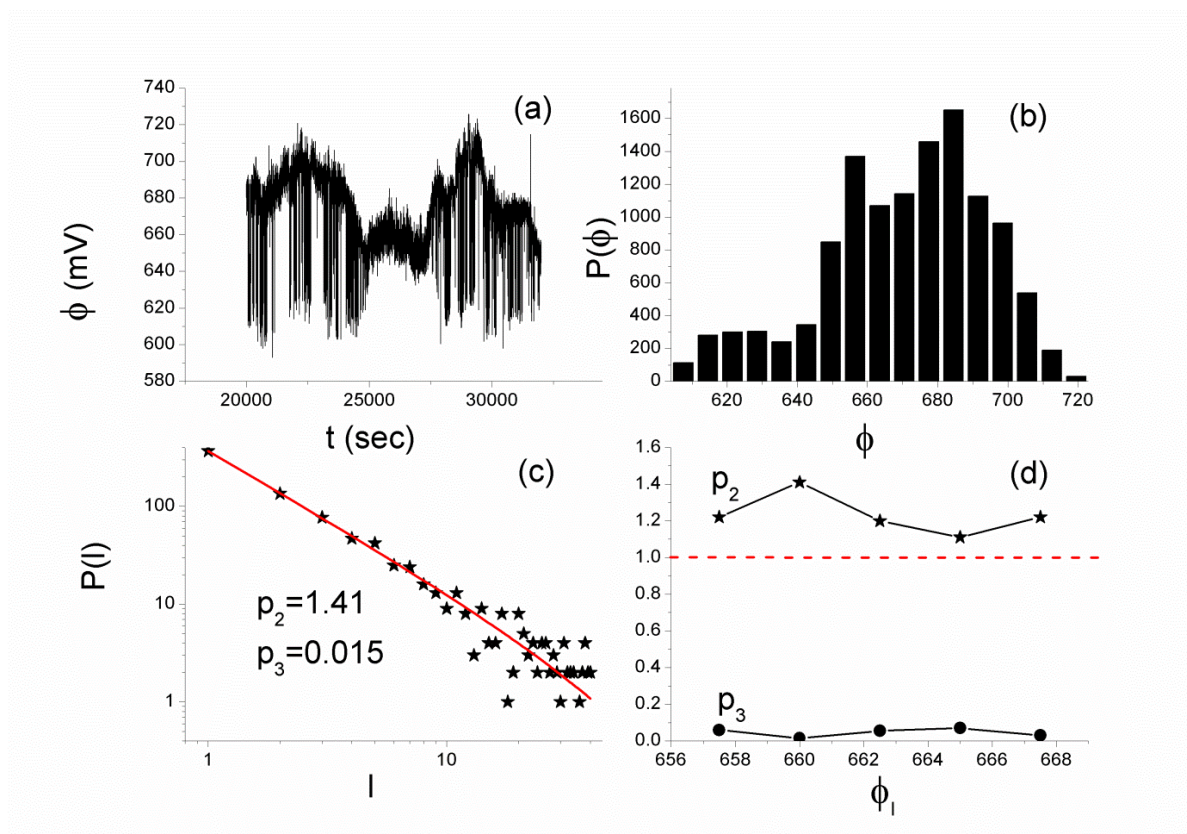
10



1

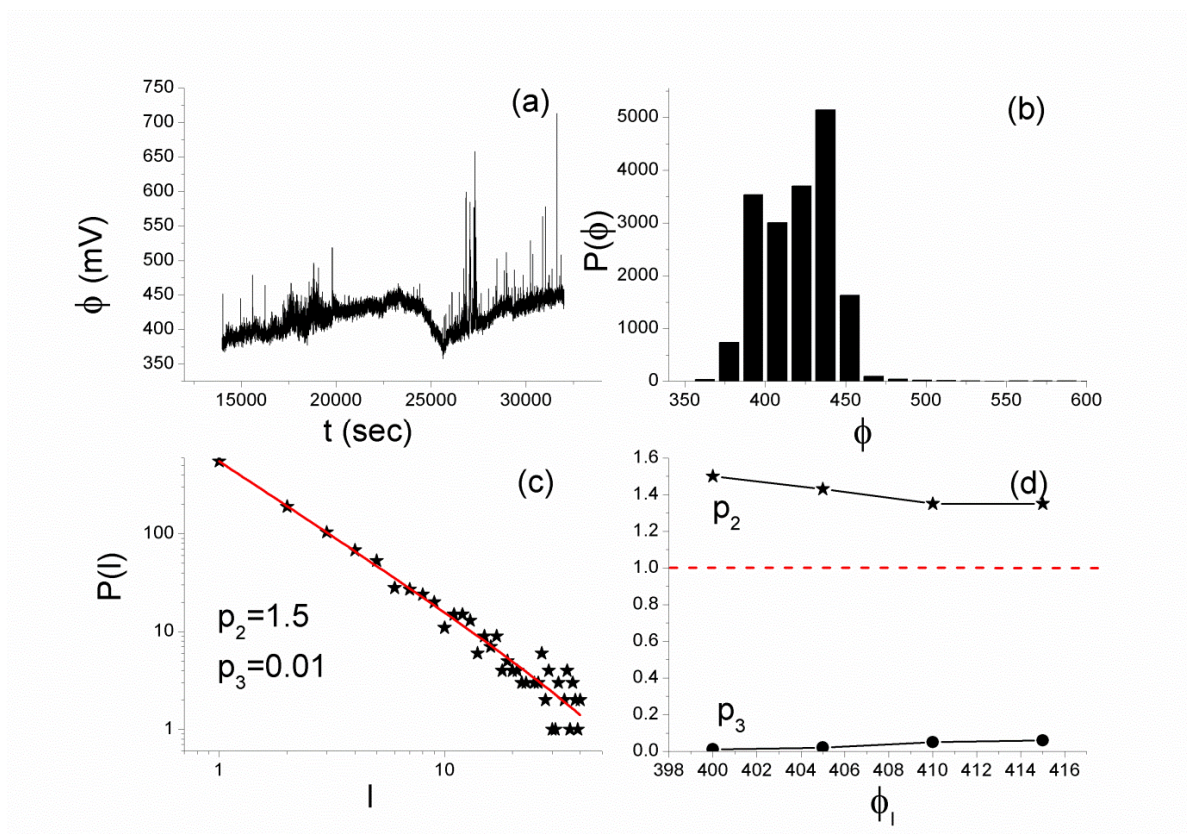
2 **Figure 3.** (a) The 10,000 samples long critical window of the MHz EME that was recorded
 3 prior to the Cephalonia $M_w = 6.0$ EQ at the Zante station, while (b), (c), and (d) are similar to
 4 the corresponding parts of Fig. 2. From 3b, a fixed-point (start of laminar regions), ϕ_o of
 5 about 600 mV results, while in Fig. 3c, the distribution of laminar lengths is given for the end
 6 point $\phi_l = 665mV$ for which the exponents $p_2 = 1.49$, $p_3 = 0.000$ with $R^2 = 0.999$ were
 7 obtained.

8



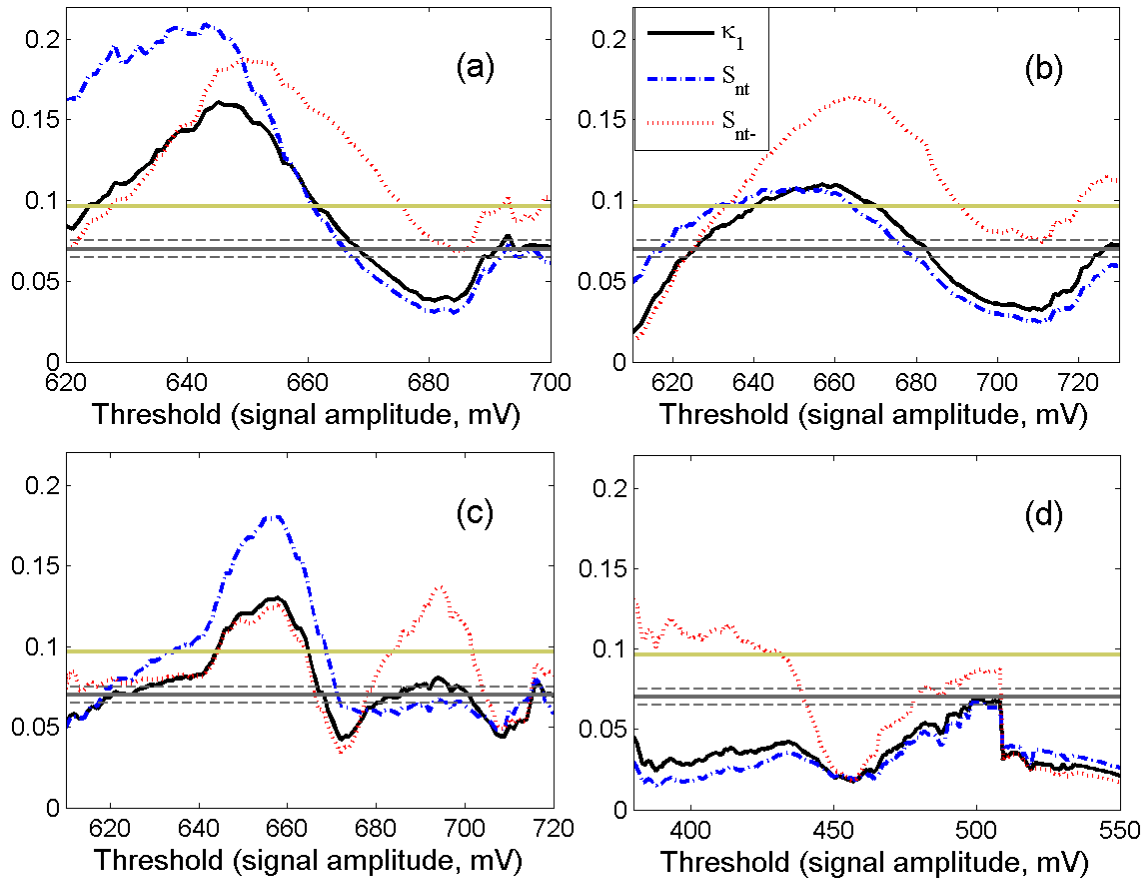
1
 2 **Figure 4.** (a) The 12,000 samples long critical window of the MHz EME that was recorded
 3 before the Cephalonia $M_w = 5.9$ EQ at the Cephalonia station, while (b), (c), and (d) are
 4 similar to the corresponding parts of Fig. 2. In Fig. 4c, the distribution of laminar lengths is
 5 given for the end point $\phi_l = 660mV$.

6



1
 2 **Figure 5.** (a) The 18,000 samples long critical window of the MHz EME that was recorded
 3 before the Cephalonia $M_w = 5.9$ EQ at the Zante station; (b), (c), and (d) are similar to the
 4 corresponding parts of Fig. 2. In Fig. 5c, the distribution of laminar lengths corresponds to the
 5 end point $\phi_l = 400mV$.

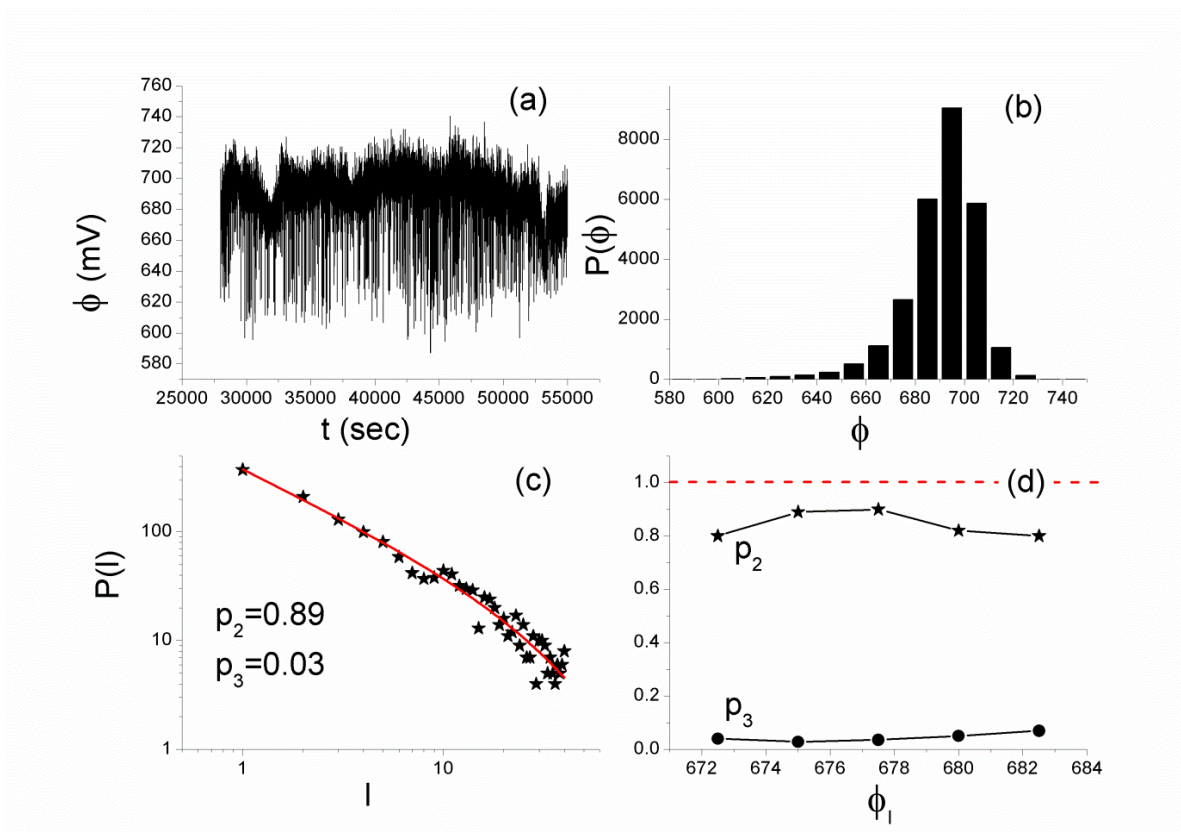
6



1

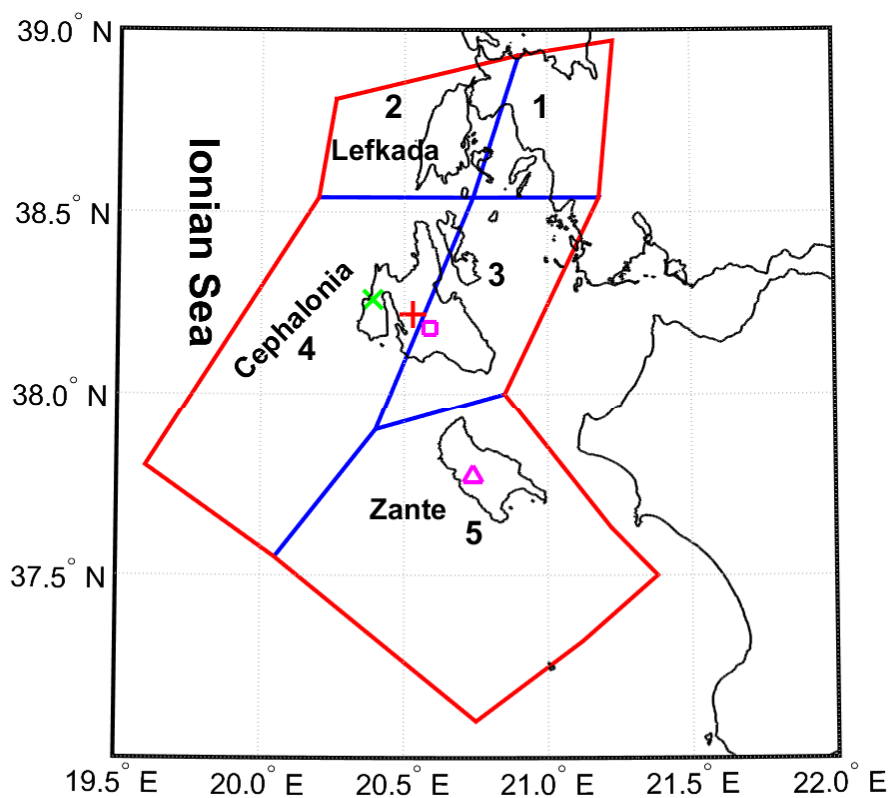
2 **Figure 6.** Natural time analysis results obtained for the MHz EME signals shown in: (a) Fig.
 3 2a, recorded at Cephalonia station prior to EQ1, (b) Fig. 3a, recorded at Zante station prior to
 4 EQ1, (c) Fig. 4a, recorded at Cephalonia station prior to EQ2, and (d) Fig. 5a, recorded at
 5 Zante station prior to EQ2. The quantities κ_1 (solid curve), S_{nt} (dash-dot curve), and S_{nt-}
 6 (dot curve) vs. amplitude threshold for each MHz signal are shown. The entropy limit of
 7 $S_u (\approx 0.0966)$, the value 0.070 and a region of ± 0.005 around it are denoted by the
 8 horizontal solid light green, solid grey and the grey dashed lines, respectively. (For
 9 interpretation of the references to colors, the reader is referred to the online version of this
 10 paper.)

11

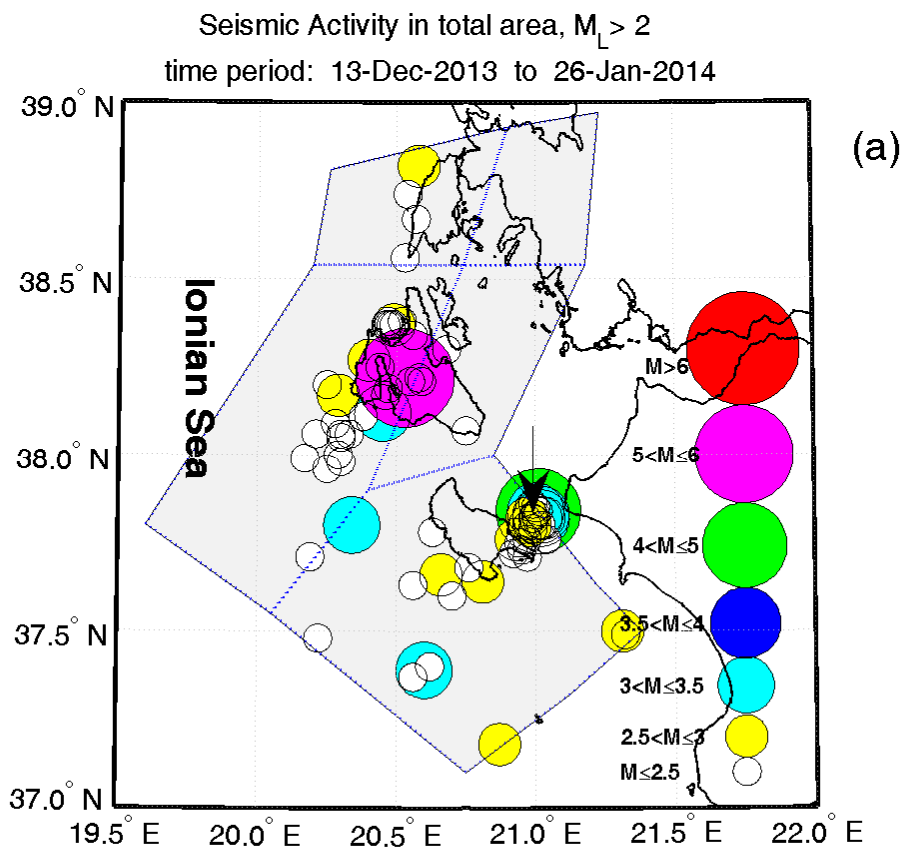


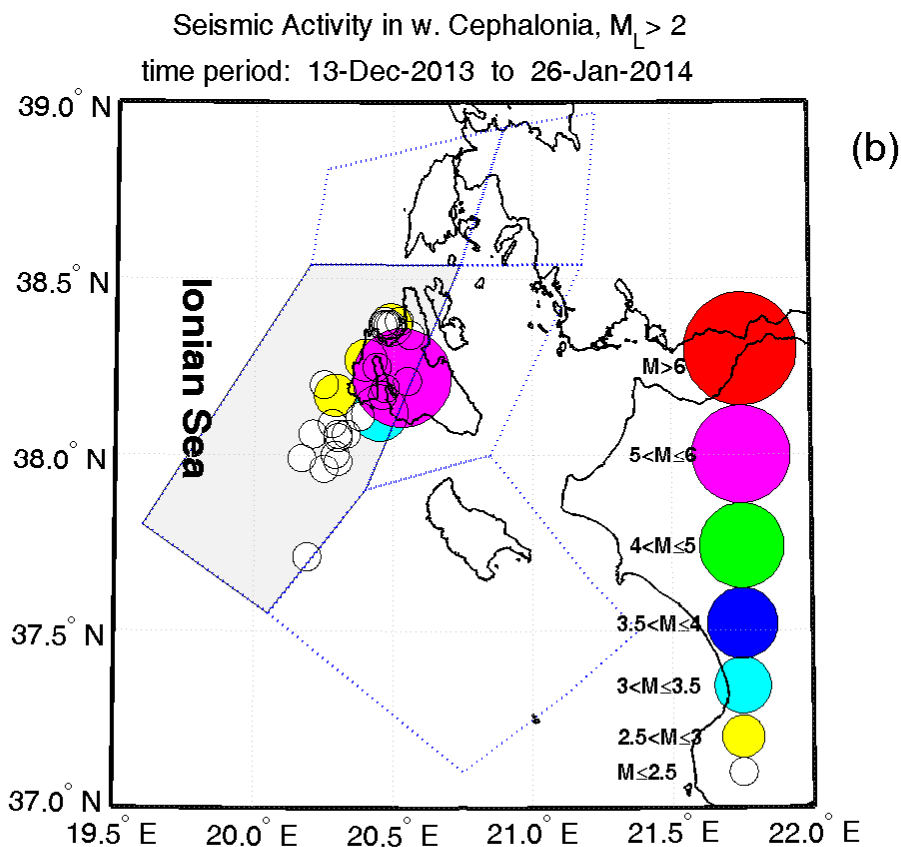
1
 2 **Figure 7.** (a) The 27,000 samples long tricritical excerpt of the Mhz EME that was recorded
 3 before the Cephalonia $M_w = 5.9$ EQ at the Cephalonia station; (b), (c), and (d) are similar to
 4 the corresponding parts of Fig. 2. In Fig. 7c, the distribution of laminar lengths corresponds to
 5 the end point $\phi_l = 675mV$.

6



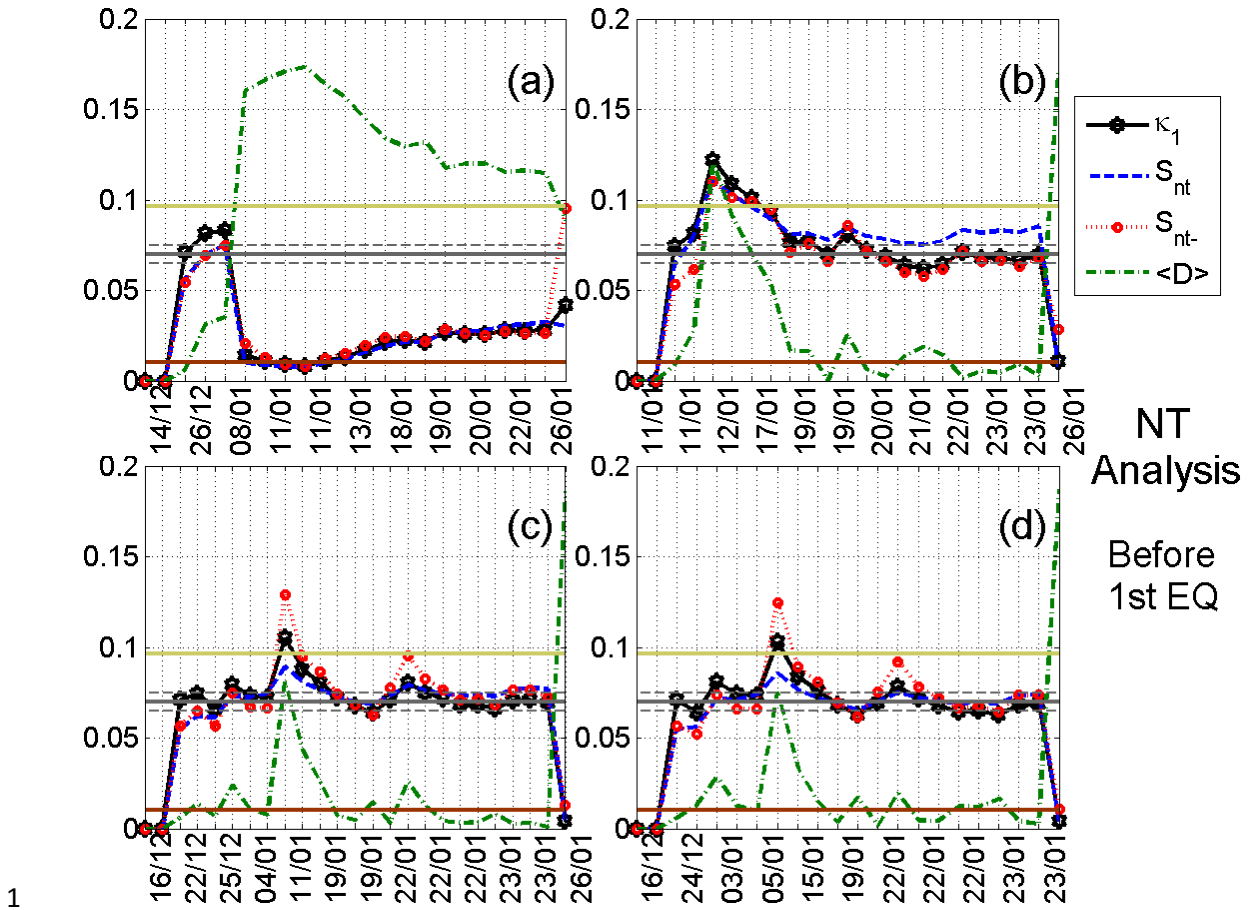
1
 2 **Figure 8.** Seismic zonation in the Ionian Islands area. The locations of the Cephalonia and
 3 Zante stations, as well as the epicenters of the two significant EQs of interest are marked,
 4 using the same signs presented in Fig. 1.
 5





1
 2 **Figure 9.** Foreshock seismic activity (M_L) before EQ1: (a) for the whole investigated area of
 3 the Ionian Sea region; (b) for west Cephalonia. (For interpretation of the references to colors,
 4 the reader is referred to the online version of this paper.)

5

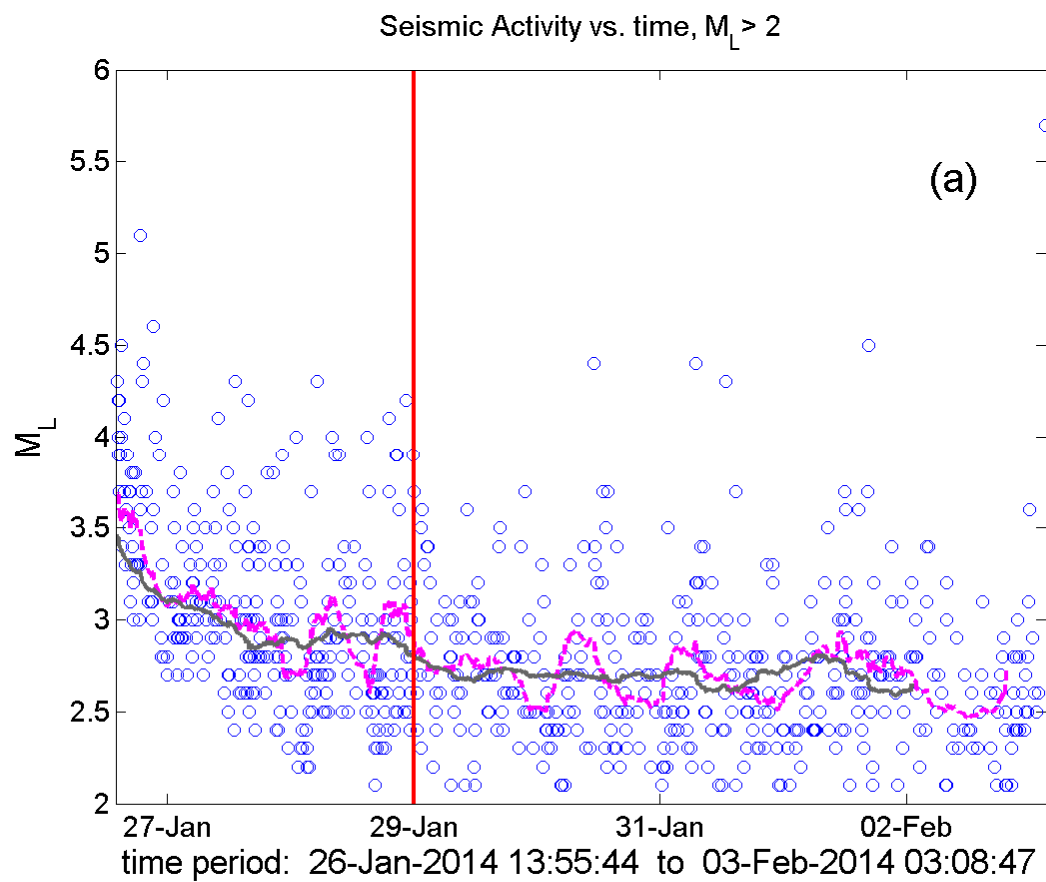


1
2 **Figure 10.** Temporal evolutions of the four natural time (NT) analysis parameters (κ_1 , S_m ,
3 S_{m-} , and $\langle D \rangle$) for the foreshock seismic activity recorded prior to EQ1: (a) for the activity of
4 the whole investigated area of the Ionian Sea for M_L threshold 2.5, during the period from
5 13/12/2013 00:00:00 to 26/01/2014 13:55:44 UT (just after the occurrence of EQ1); (b) for
6 the activity of the whole investigated area of the Ionian Sea for M_L threshold 2.3, during the
7 period from 11/01/2014 04:13:00 (just after the $M_L = 4.7$ occurred in Zante) to 26/01/2014
8 13:55:44 UT; (c) for the activity of both Cephalonia (east and west) zones combined for M_L
9 threshold 2.1, during the period from 13/12/2013 00:00:00 to 26/01/2014 13:55:44 UT;. (d)
10 for the activity of the west Cephalonia for M_L threshold 2.1, during the period from
11 13/12/2013 00:00:00 to 26/01/2014 13:55:44 UT. Note that the events employed depend on
12 the considered threshold. Moreover, the time (x-) axis is not linear in terms of the
13 conventional date of occurrence of the events, since the employed events appear equally
14 spaced relative to x-axis, as the natural time representation demands, although they are not

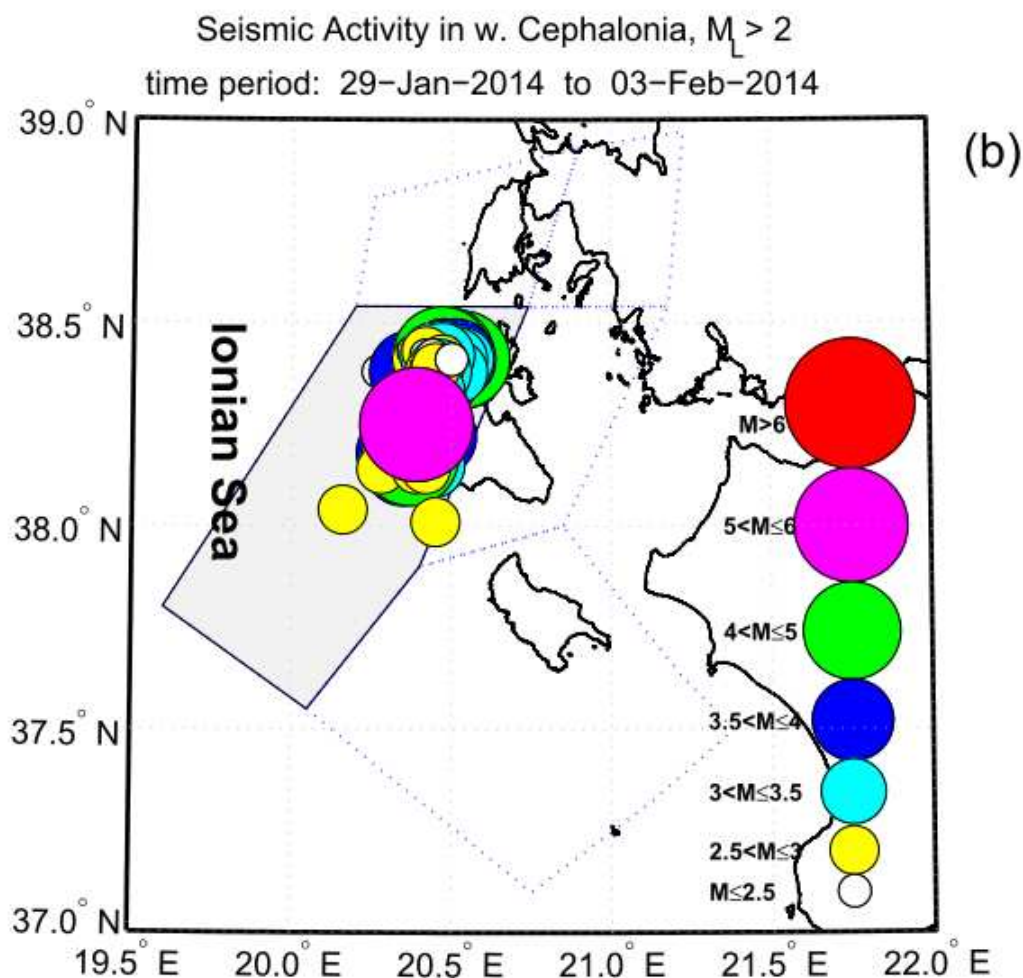
1 equally spaced in conventional time. The horizontal solid light green, solid grey and the grey
2 dashed lines, denote the same quantities as in Fig. 6, while the horizontal solid brown line
3 denotes the 10^{-2} limit for $\langle D \rangle$. (For interpretation of the references to colors, the reader is
4 referred to the online version of this paper.)

1

2



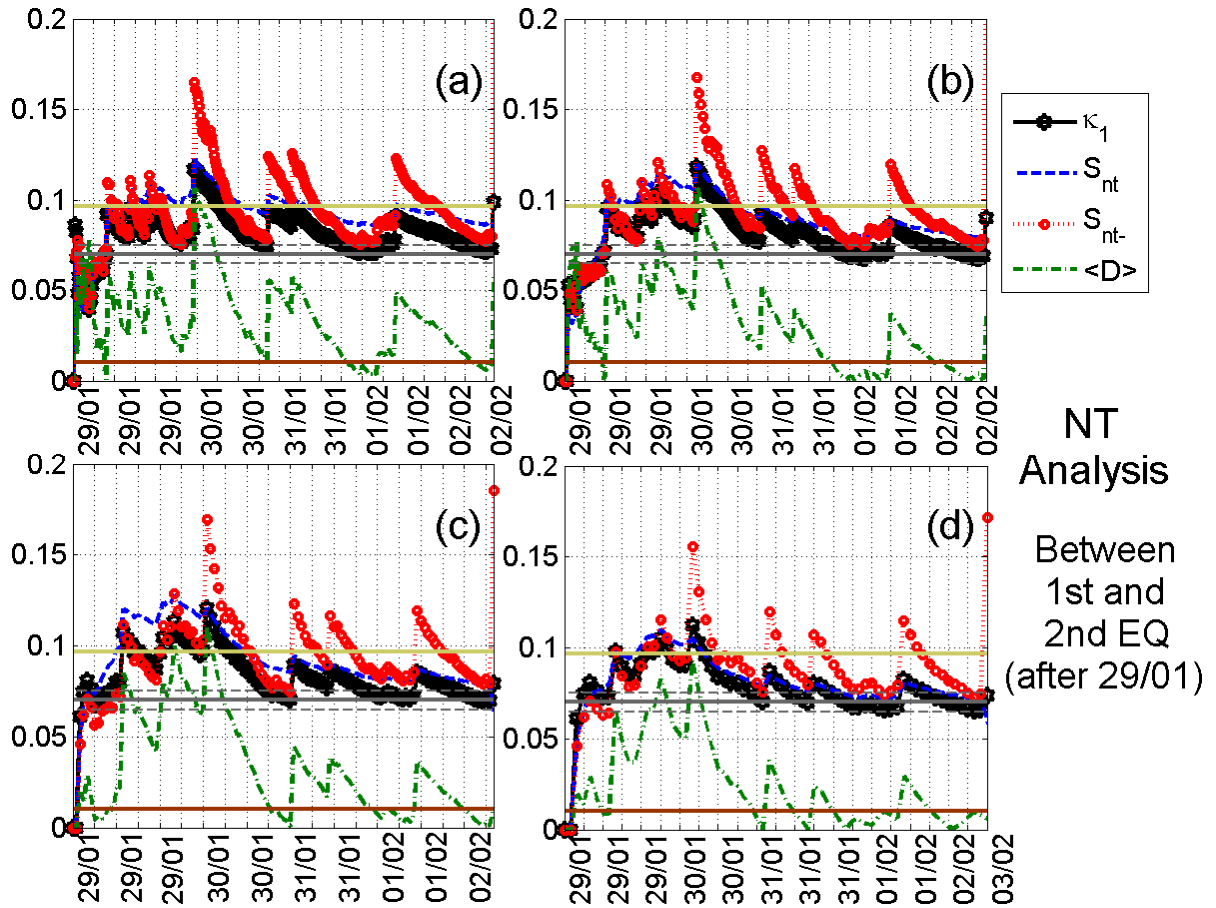
3



1

2 **Figure 11.** (a) Seismic activity from the time immediately after EQ1 ($M_w = 6.0$) up to the
 3 time of EQ2 ($M_w = 5.9$) for the whole investigated area of the Ionian Sea. The moving
 4 averages of the recorded earthquake local magnitudes vs. time for calculation windows of 25
 5 and 75 successive events are shown by the dashed magenta and solid grey curve, respectively.
 6 The vertical solid red line denotes the time point 29 January 00:00:00 UT. (b) The considered
 7 as foreshock seismic activity before EQ2 (from 29/01/2014 00:00 UT up to the time of
 8 occurrence of EQ2) for west Cephalonia. All presented magnitudes are local magnitudes
 9 (M_L). (For interpretation of the references to colors, the reader is referred to the online
 10 version of this paper.)

11



1
 2 **Figure 12.** Natural time (NT) analysis results for the seismicity in the partition of west
 3 Cephalonia during the time period from 29/01/2014 00:00:00 to 03/02/2014 03:08:47 UT
 4 (between EQ1, $M_w = 6.0$, and EQ2, $M_w = 5.9$): (a)-(d) Temporal evolutions of the four
 5 natural time analysis parameters (κ_1 , S_{nt} , S_{nt-} , and $\langle D \rangle$) for the different M_L thresholds 2.2,
 6 2.6, 2.8, and 3.0, respectively. Note that the events employed depend on the considered
 7 threshold. Moreover, the time (x-) axis is not linear in terms of the conventional date of
 8 occurrence of the events, since the employed events appear equally spaced relative to x-axis,
 9 as the natural time representation demands, although they are not equally spaced in
 10 conventional time. The horizontal solid light green, solid grey and the grey dashed lines,
 11 denote the same quantities as in Fig. 6, while the horizontal solid brown line denotes the 10^{-2}
 12 limit for $\langle D \rangle$. (For interpretation of the references to colors, the reader is referred to the
 13 online version of this paper.)